The diverse structural modes of tRNA binding and recognition

Received for publication, February 15, 2023, and in revised form, June 20, 2023 Published, Papers in Press, June 26, 2023,
https://doi.org/10.1016/j.jbc.2023.104966

Anna Biela[1,‡], Alexander Hammermeister[1,‡], Igor Kaczmarczyk[1,2,‡], Marta Walczak[1,2,‡], Lukasz Koziej[1,‡], Ting-Yu Lin[1,*], and Sebastian Glatt[1,*]

From the [1]Malopolska Centre of Biotechnology, and [2]Doctoral School of Exact and Natural Sciences, Jagiellonian University, Krakow, Poland

Reviewed by members of the JBC Editorial Board. Edited by Karin Musier-Forsyth

tRNAs are short noncoding RNAs responsible for decoding mRNA codon triplets, delivering correct amino acids to the ribosome, and mediating polypeptide chain formation. Due to their key roles during translation, tRNAs have a highly conserved shape and large sets of tRNAs are present in all living organisms. Regardless of sequence variability, all tRNAs fold into a relatively rigid three-dimensional L-shaped structure. The conserved tertiary organization of canonical tRNA arises through the formation of two orthogonal helices, consisting of the acceptor and anticodon domains. Both elements fold independently to stabilize the overall structure of tRNAs through intramolecular interactions between the D- and T-arm. During tRNA maturation, different modifying enzymes posttranscriptionally attach chemical groups to specific nucleotides, which not only affect translation elongation rates but also restrict local folding processes and confer local flexibility when required. The characteristic structural features of tRNAs are also employed by various maturation factors and modification enzymes to assure the selection, recognition, and positioning of specific sites within the substrate tRNAs. The cellular functional repertoire of tRNAs continues to extend well beyond their role in translation, partly, due to the expanding pool of tRNA-derived fragments. Here, we aim to summarize the most recent developments in the field to understand how three-dimensional structure affects the canonical and noncanonical functions of tRNA.

The need of an adapter molecule that decodes genetic information into function was predicted by Francis Crick in 1958 (1). In eukaryotes, tRNAs are transcribed by RNA Polymerase III and undergo several steps of maturation before being charged with their cognate amino acids (2, 3). Approximately 1000 individual and unique tRNA sequences have been identified by different sequencing methods in over 400,000 analyzed genomes (4). The human genome contains over 500 genes that encode functional tRNAs, which are able to decode 62 codons, including selenocysteine (4) and pyrrolysine (5). As the redundant pool of tRNAs is produced from several genomic loci, the number of clinically relevant mutations in cytoplasmic tRNA genes is relatively low (6). Nonetheless, mutations in mitochondrial tRNA genes and altered expression levels of individual tRNAs are associated with various human diseases (7, 8). Numerous reports of patient-derived mutations in genes coding for tRNA maturation, processing, and modification enzymes directly highlight the importance of accurate tRNA biogenesis for human health and disease (9–14). Recently, tRNAs have been rediscovered as potential therapeutics to readjust protein synthesis in specific diseases (15). This idea has sparked interest from various research groups and highlights the importance of revisiting the structure of these small RNAs.

The general structure and shape of tRNAs

tRNA is a biopolymer composed of 76 to 90 RNA nucleotides (nt) linked together *via* 3'-5' phosphodiester bonds (16). Each nucleotide consists of a phosphate group attached *via* an ester bond to a five-carbon sugar (ribose), which is linked to one of the four nitrogenous bases, namely the purines (adenine and guanine) or the pyrimidines (uracil and cytosine). Specific hydrogen bonding networks between the bases define the characteristic clover-leaf secondary structure of tRNA, which was already predicted from the first sequence of yeast $tRNA^{Ala}_{AGC}$ determined in 1965 by Holley *et al.* (17). The canonical secondary structure of tRNAs is divided into the following domains (Fig. 1*A*): (i) acceptor stem (also known as amino acid accepting stem (AAS) or acceptor arm) linked *via* (ii) the 2-nt "connector" to the (iii) D-stem loop (D-arm) closed by the D-loop, (iv) anticodon stem loop (ASL, anticodon arm), (v) variable region (variable loop, variable arm), and (vi) T-stem loop (T-arm or TΨC-arm) (18). The 3' terminus includes a single-stranded CCA sequence (19), which constitutes the site of covalent amino acid attachment during aminoacylation (20). Nucleotides are numbered from 5' to 3', and the posttranscriptionally added nucleotides are indicated by the number of the preceding nucleotide followed by a colon and a letter in alphabetical order. From extensive sequencing data, we know that U_8, A_{14}, G_{18}, G_{19}, A_{21}, U_{33}, G_{53}, T_{54}, Ψ_{55}, C_{56}, A_{58}, C_{61}, C_{74}, C_{75}, and A_{76} are the most conserved nucleotides within tRNAs. Y_{11}, R_{15}, R_{24}, Y_{32}, R_{37}, Y_{48}, R_{57}, and Y_{60}

‡ These authors contributed equally to this work.
* For correspondence: Sebastian Glatt, sebastian.glatt@uj.edu.pl; Ting-Yu Lin, ting-yu.lin@uj.edu.pl.

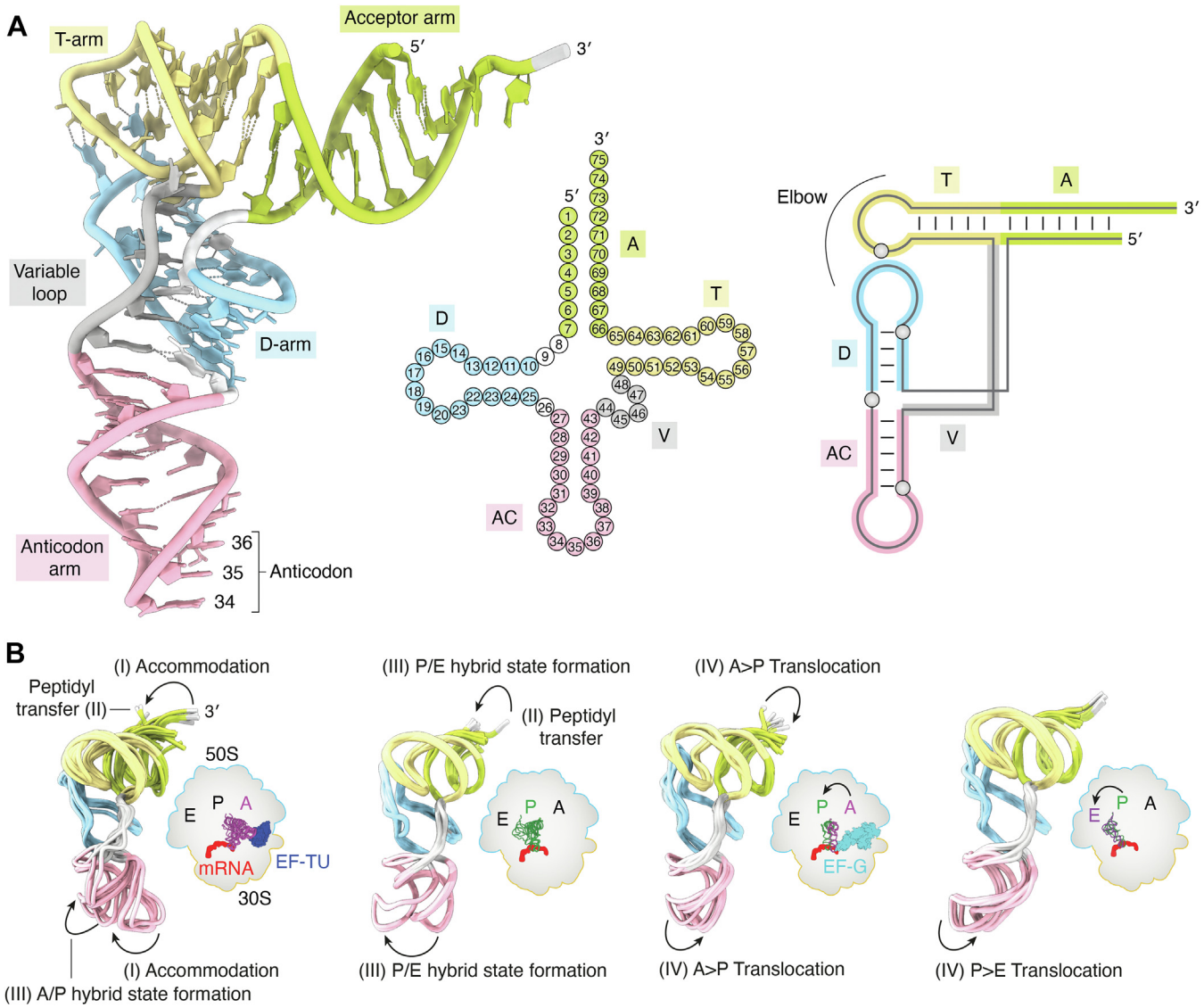

Figure 1. The structure of tRNA at different levels and during translation. *A*, *left*: specific regions are indicated on yeast $tRNA^{Phe}_{GAA}$ (PDB ID 1EHZ) as follows: 3' and 5' end; acceptor arm (*light green*); T-arm (*yellow*); D-arm (*light blue*); variable loop (*gray*); anticodon arm (*pink*); and 34, 35, 36 anticodon nt. The dimensions of folded tRNAs are approximately 60 × 70 × 25 Å. *Middle*: clover-leaf secondary structure representation of tRNA numbered according to the standard convention. *Right*: tertiary nucleotide interactions responsible for the L-shape tRNA structure. *B*, multiple structures of tRNA extracted from the context of elongating bacterial 70S ribosome determined by time-resolved cryo-EM. The schematic demonstrates local flexibility of the A-site (*magenta*), P-site (*dark green*), and E-site (*purple*) tRNA associated with the cognate mRNA (*red*) bound to the 70S ribosome [large 50S (*blue*) and small 30S (*orange*)]. The *arrows* highlight the bending of the 3' end (*silver*) from the acceptor arm (*light green*) and the swinging of the anticodon arm (*pink*). The major sequential steps of the elongation cycle associated with the L-shape distortion are indicated with Roman numerals (I–IV). The two superimpositions on the *left* (A-site phenylalanine- and P-site methionine-tRNA) follow the steps and changes after cognate aminoacyl-tRNA delivery by elongation factor EF-TU (*dark blue*). The two superimpositions on the *right* depict AP proline- and PE methionine-tRNA translocation facilitated by elongation factor EF-G (*cyan*), which resets the system for the next elongation cycle. EF-Tu, Elongator factor-Tu.

(R = purine; Y = pyrimidine) are semiconserved nucleotides found in many tRNA sequences. Differences in tRNA length are mainly a consequence of the varying sequence length in the variable loop that can accommodate "extra" nucleotides, while preserving the overall domain organization and three-dimensional shape (21). Some exceptions to the clover-leaf secondary structure are found in mammalian mitochondrial tRNAs (22, 23), flagellates (24), and nematodes (25, 26). In these rare cases, deviations occur in the D-stem/loop or T-stem/loop architecture or the complete D-loop is lacking (18, 27), which will be described in the following sections.

The secondary structure of tRNAs not only depends on the RNA nucleotide sequence itself but also on the presence of other additional factors. For instance, coordination of magnesium ions is required for correct folding of $tRNA^{Glu}_{UUC}$ in *Escherichia coli* (28). Despite sequence variations, all tRNAs fold into the characteristic L-shaped three-dimensional tertiary structure (29) (Fig. 1*A*). This compact shape comprises two orthogonal helical branches, each containing several Watson-Crick base pairs (bp). In detail, the AAS is stacked over the T-stem loop to form the acceptor domain that is linked by the so-called "elbow" region (30) to the anticodon domain formed

by ASL and D-stem loop. The L-shape is further stabilized by additional non-Watson-Crick interactions between D- and T-arms. This uniform L-shaped conformation was initially proposed in 1974 based on the first crystal structure of yeast $tRNA^{Phe}_{GAA}$ (31–34) and then confirmed by other structural studies of yeast $tRNA^{Asp}_{GUC}$ (35, 36), bacterial (37) and yeast (38) initiator $tRNA^{Met}_{CAU}$, and human $tRNA^{Lys}_{UUU}$, the primer of HIV reverse-transcriptase (39). The correct folding, stability, and functionality of tRNAs are also influenced by the posttranscriptional incorporation of chemical modifications (40).

Individual regions of tRNAs

In general, the size of acceptor (AAS), anticodon, and T-arms are highly conserved among functional tRNAs. The AAS is composed of a stem that is formed between the first 7 nt (5' end) and nt 66 to 72 (3' end), creating a molecular zipper (Fig. 1*A*). It is completed by a 4-nucleotide long, single-stranded overhang, harboring the so-called discriminator base at position 73 (41) followed by the CCA-tail. The exceptions to this general principle are all $tRNA^{His}_{GUG}$, which contain a posttranscriptionally added guanine nucleotide at the 5' end, numbered "0" or "–1" (42). The discriminator base is one of the major identity elements that, in combination with several other nucleotides in the anticodon and the acceptor helix, ensures the very high specificity of aminoacyl-tRNA synthetases (43, 44). During the maturation process, 5' leader sequences are excised by the endonuclease RNase P (45) prior to the 3' trailer, although this order can be reversed for tRNAs harboring long 3' trailer sequences (46). In the case of the 3' end, the CCA sequence can be encoded in the tRNA gene (*e.g.*, *E. coli* and related bacteria, certain Gram positive bacteria) or added to the tRNA during a separate maturation process in eukaryotes, certain Gram positive bacteria, and archaea (47). In the first scenario, 3' trimming is primarily carried out by the exoribonucleases RNase T and RNase PH (48), but other exoribonucleases (*e.g.*, RNase II and RNase D or RNase BN (49)) can act as a substitute, if needed. When the CCA is not encoded in the genomic sequence, the 3' endonuclease RNase Z initially cleaves the overhang after the discriminator base and leaves a 3'-OH group (50); subsequently the tRNA nucleotidyltransferase adds the 3′ terminal CCA residues without the need of a template (51). The fundamental role of the CCA sequence is to allow aminoacylation and therefore provide a charged tRNA to the ribosome. Moreover, inside the ribosome, the CCA sequence enables dynamic interactions with ribosomal proteins and rRNA elements as the tRNA is moved through the ribosome (52, 53) (Fig. 1*B*).

The 5' end of the acceptor stem is connected to the D-arm by two nt (U_8 and N_9), which represents the second most variable region of tRNAs (Fig. 1*A*). The D-arm derives its name from the dihydrouridine (D) modification present at the 3' and/or 5' of conserved G_{18} and G_{19}. Typically, the D-arm comprises a 4-bp stem (positions 10–13 pair with 22–25) that ends in a 7–11 nucleotide loop containing conserved nt A_{14}, A_{21}, G_{18}, and G_{19}. The 3' part of the acceptor arm is directly connected to the T-arm, which is typically a 5-bp long stem (positions 61–65 pair with 49–53) with a loop composed of seven nt (positions 54–60). Due to the presence of a universally conserved motif [thymidine 54, pseudouridine (Ψ) 55, and cytosine 56], it is also called the "TΨC-arm". C_{56} and $Ψ_{55}$ form interactions with conserved residues G_{19} and G_{18} in the D-arm, which stabilizes the L-shaped form of tRNA (54). The D-arm is also responsible for interactions with the ribosome during all stages of translation (55).

The variable region, as its name indicates, can vary in length (56). In type I tRNAs, it usually consists of four or five nt, whereas in type II tRNAs (*e.g.*, $tRNA^{Ser}$, $tRNA^{Leu}$, $tRNA^{Tyr}$), it consists of 10 to 24 nt. The longer variable regions are arranged in a double helical stem of 3 to 7 bp and a loop of 4 to 5 nt. Nucleotides in the variable region are located between position 45 and 46 and obey canonical base-pairing rules. The nt in the 5'-strand and the 3'-strand are numbered e11, e12, e13,... and e21, e22, e23,..., respectively. The prefix 'e' is specific for the variable region, and the second digit identifies the respective base-pair. In the case of a long variable region, the loop can be formed by up to 5 nt: e1, e2, e3, e4, and e5 (57).

The anticodon arm consists of a 5-bp stem (positions 27–31 pair with 39–43) and a 7-nt loop (positions 32–38), containing U_{33}, R_{37}, and the anticodon triplet N_{34}, N_{35}, N_{36}. The anticodon, together with a discriminator base, is one of the main identity elements of tRNAs (58). It is responsible for reading codon triplets in mRNAs and 61 different sense codons encoding 20 standard amino acids. The 21st amino acid, selenocysteine, is recoded by the UGA stop codon if assisted by a specific selenocysteine insertion sequence elements in the mRNA and is directly synthetized on already charged $tRNA^{Ser}_{UCA}$ (59, 60). The 22nd amino acid, pyrrolysine, was discovered in *Methanosarcina barkeri* and is encoded by an UAG codon in the methylamine methyltransferase genes (61). The number of tRNA species in different organisms varies between 23 and 45, clustered in 20 groups of so-called isoacceptors. These are tRNAs that are charged with the same amino acid despite having different anticodons. Apart from methionine and tryptophan, all amino acids have multiple isoacceptors. The anticodon does not even have to be fully complementary to recognize a specific codon triplet. The nature of the wobble base at position 34 enables the accommodation of noncanonical interactions between the codon and anticodon. Furthermore, the ASL is the most heavily modified region of tRNA, with these modifications either restricting or facilitating the decoding process (62).

The overall L-shape of tRNA is maintained even though conformational changes occur during the different steps of the ribosomal translation cycle (Fig. 1*B*). Advances in time-resolved cryo-EM (63) have allowed the structural visualization of distinct states of the ribosome and tRNAs during translation (64, 65). The characteristic L-shape of tRNAs is further substantiated by numerous examples of structural "mimicry", where other RNAs or proteins adopt a tRNA-like shape (66). For instance, viruses use the tRNA-shaped internal ribosome entry site in order to recruit ribosomes to initiate translation at non-AUG codons (67, 68). Furthermore,

Staphylococcus aureus uses a riboswitch (*yjdF*) that was found to mimic the overall shape of a tRNA to activate translation (69). The translational elongation and ribosome recycling factors (*e.g.*, EF-G, EF2, or RRF) also use structural mimicry to specifically interact with the ribosome (70–73).

RNA modifications and their influence on the folding/stability of tRNAs

tRNAs fold into an L-shaped three-dimensional structure despite their high sequence variation (33, 74). At first glance, one would simply assume that the available sequences provide sufficient constraints for all tRNA transcripts to adopt the L-shaped conformation. This notion is also supported by very similar crystal structures of modified and unmodified tRNA-$^{Phe}_{GAA}$ from bacteria and eukaryotes (Fig. 2*A*) (74–77). Several studies indeed have demonstrated that various "naked" *in vitro*–transcribed tRNAs are able to fold into functional L-shaped tRNAs that can be charged by aminoacyl-tRNA synthetases or used in *in vitro* translation systems (78–81). However, other unmodified tRNA transcripts are found to dynamically switch between multiple conformations, and the equilibrium between misfolded and properly folded forms is regulated by additional factors, such as modifications or environmental conditions (82). For instance, unmodified human mitochondrial tRNA$^{Lys}_{UUU}$ displays as an extended bulged-hairpin structure instead of the canonical cloverleaf structure. This finding is consistent with the observation that some hypomodified tRNAs are not functional *in vivo* and subject to degradation (83–89). Approximately 100 different RNA modifications are found in tRNAs, and on average ~17% of nt are modified in each tRNA molecule (90–92). The occurrence of tRNA modifications can be divided into two groups, based on their functionality within the molecule: (i) modifications that are involved in the process of translational decoding and (ii) those that control tRNA folding and stability (91, 93, 94).

In light of excellent reviews focusing on tRNA modifications (27, 40, 62, 95–99), we focus here on those modifications that seem important for the core structure of tRNA$^{Phe}_{GAA}$ in prokaryotes and eukaryotes. In general, modifications that affect the tertiary structure of tRNA are rather simple, such as reduction or isomerization of uridine to D or Ψ, methylation of the base and/or ribose sugar, replacement of oxygen on the base with sulfur, or the addition of small functional groups, like aminocarboxypropylation (acp) (Fig. 2*B*) (91, 93, 100). These modifications modulate the structural plasticity of the tRNA core, where some regions become rigid and others are more flexible (75, 87, 101–103). These changes are achieved through increased hydrophobicity, change of charge, and stabilization of a 2'-*endo* or 3'-*endo* sugar conformation (87, 103–108). Depending on the position on the nucleotide, modifications can alter hydrogen bonding interactions on all three edges (Watson-Crick, Hoogsteen, and sugar-edge), which in turn can change the base-pairing properties, leading to local or global structural rearrangements of the tRNA (85, 107, 109, 110). The introduction of small chemical groups typically maximizes the stabilizing effect while minimizing the entropic penalty of attaching larger chemical groups, which are more common in the anticodon region.

One of the most prevalent tRNA modifications is methylation, which can occur on the oxygen of the 2'-OH moiety (2'-OMe), on nearly all nitrogen sites of the nucleobase (with the exception of the *N*7 and *N*3 position of adenosine) and on the *C*2/*C*5 atom of pyrimidines and adenosine (104, 111, 112). The presence of a 2'-OMe group induces the 3'-*endo* ribose conformation, through repulsion between the 2'-OMe and 3'-phosphate, resulting in the stabilization of an A-form helical region (104, 106, 112). This effect leads to an increased melting temperature of tRNA and decreased susceptibility to alkaline and enzymatic hydrolysis (109, 113, 114). Methylations on the Watson-Crick edge appear predominantly on the 5'-side of the tRNA and prevent canonical base pairing (40, 104). The m^1A modification at position 9 and 58 is common and has been linked to correct folding and structural stability of tRNA (85, 115). A prime example for global structural rearrangement is the well-studied m^1A_9 modification in human mitochondrial mt-RNA$^{Lys}_{UUU}$. It was shown that mt-RNA$^{Lys}_{UUU}$ exists in an equilibrium between the classical L-shaped and an alternative extended hairpin conformation. Addition of the methyl group to *N*1 of adenosine disrupts A_9-U_{64} base pairing, which supports the hairpin conformation and shifts the equilibrium towards the correctly folded structure through A_{50}-U_{64} pairing (85, 115, 116). A similar effect was also described for mt-RNA$^{Asp}_{GUC}$ and mt-RNA$^{Leu}_{UUR}$, demonstrating the importance of modifications for mitochondrial tRNA folding (117–121). Methylation of *N*1 at guanosine 9 (m^1G9) in cytoplasmic and mitochondrial tRNAs also disrupts canonical base pairing and is believed to be involved in structural reorganization (122, 123). The *N*1-methylation of A_{58} does not disrupt the reverse-Hoogsteen base pairing with T_{54} but introduces a positive charge that stabilizes the base pairing and thus the tertiary structure (124–128).

Single or double methylation of *N*2 in guanosine (m^2G, $m^2{}_2G$) occurs frequently in the junctions between acceptor stem and D-arm (position 9 and 10) as well as between the D-arm and anticodon loop (position 26 and 27) in some eukaryotic and some bacterial tRNAs (129–134). m^2G can also be found at position 6 and 7 in the acceptor stem of higher eukaryotes (133, 135). The single methyl group on *N*2 of G_{10} does not interfere with the triple base pairing between G_{10}-C_{25}-G_{45}, but the hydrophobic character of the methyl group might stabilize the D-loop (132, 136). Dimethylation of G_{26} prevents base pairing with cytidine but still allows pairing with any other nucleotide (132, 137). Similar to m^1A_9, it was shown that $m^2{}_2G26$ prevents an alternative folding of the human cytosolic tRNA$^{Asn}_{GUU}$ (137). Interestingly, $m^2{}_2G_{26}$ prevents mispairing with C_{11} and controls pairing with A_{44}, which contributes to the stabilization of the hinge region between the D-arm and anticodon loop (132, 134, 137, 138).

The most prominent methylation on the 3'-half of tRNAs is m^5U_{54}/T or ribothymidine, and it occurs in the T-loop of nearly all tRNAs. m^5U_{54} together with m^1A_{58} forms a reverse-Hoogsteen bp, which stabilizes the T-arm through additional

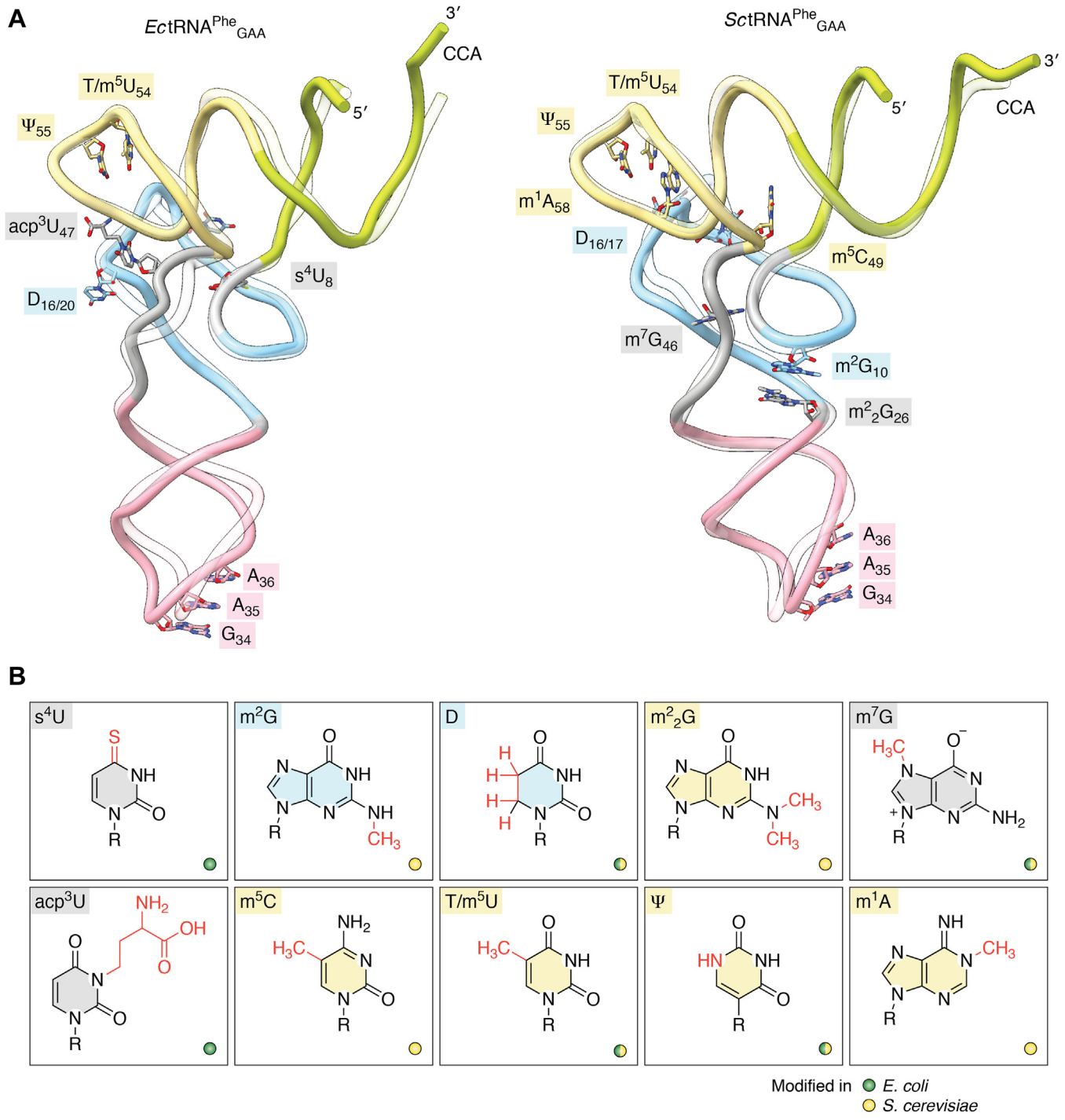

Figure 2. Structure of unmodified and modified tRNA^{Phe}. *A*, comparison of prokaryotic and eukaryotic tRNA$^{Phe}_{GAA}$. Superimpositions of *in vitro* transcribed (*transparent*) and endogenous (*opaque*) tRNA$^{Phe}_{GAA}$ from *Escherichia coli* (*Ec*) and *Saccharomyces cerevisiae* (*Sc*) obtained by crystallography. These tRNAs are depicted as cartoons using the same color code for each region as in Figure 1. Modifications that are important for the tRNA core structure are represented in *sticks* and colored according to their position in the tRNA. The PDB IDs and resolution limits of each tRNA are as follows: unmodified *Ec*tRNA (PDB ID 3L0U at 3.0 Å) and *Sc*tRNA (PDB ID 5AXM at 2.2 Å) and modified *Ec*tRNA (PDB ID 6Y3G at 3.1 Å) and *Sc*tRNA (PDB ID 1EHZ at 1.9 Å). The m^{7}G$_{47}$ modification in *Ec*tRNA (PDB ID 6Y3G) is present in tRNA$^{Phe}_{GAA}$ but is not visible in the electron density map. *B*, chemical structures of modified nucleosides that are shown in (*A*). The modifications are indicated in *red* and the ribose moiety is annotated with R. Base colors correspond to the modified target positions in (*A*), while the color (*green* or *yellow*) of the *small circle* indicates the presence of modification in *E. coli* or *S. cerevisiae*. RMSD values for *E. coli* tRNA^{Phe} and *S. cerevisiae* tRNA^{Phe} were calculated with ChimeraX using the backbone atoms of nt 3 to 74. *E. coli*: overall RMSD 2.669 Å^2, acceptor stem 4.426 Å^2, D-arm 1.595 Å^2, anticodon-loop 2.716 Å^2, variable loop 2.362 Å^2, T-arm 1.349 Å^2; *S. cerevisiae*: overall RMSD 1.662 Å^2, acceptor stem 2.132 Å^2, D-arm 2.194 Å^2, anticodon-loop 1.628 Å^2, variable loop 0.801 Å^2, T-arm 0.665 Å^2.

base stacking with the conserved G$_{53}$-C$_{61}$ pair (125, 127, 139, 140). m^{5}C modifications between the variable loop and T-arm most likely contribute to stabilizing the tRNA core structure. In a subset of eukaryotic tRNAs, C$_{48}$ in the Levitt bp (G$_{15}$•C$_{48}$) is methylated to m^{5}C, which increases the hydrophobic character of the bp and has been suggested to promote base

stacking (40, 128, 141). Another conserved modification in the variable loop is m^7G_{46}, which introduces a positive charge that facilitates a triple base pairing with C_{13} and G_{22} and stabilizes the tertiary structure of tRNA (124, 142).

Two highly abundant uridine modifications are Ψ and D, which engender opposite structural properties. Ψ is formed through isomerization of the glycosidic bond between *N*1-*C*1 into the *C*5-*C*1 carbon-carbon bond (143–145). This repositioning alters the chemical properties of the base, resulting in a free *N*1 atom at the Hoogsteen edge that increases base-stacking properties of Ψ with its neighboring bases through the coordination of a water molecule (143–147). Furthermore, Ψ favors the 3'-*endo* sugar conformation that reinforces the local structural rigidity and stability of RNA helices (143, 144). Ψ is present at several positions in tRNA and is commonly found in position 55 in the T-loop, where it pairs with G_{18} and stabilizes the tRNA elbow region (30, 90, 148).

In contrast to Ψ and 2'-OMe that confer rigidity, D promotes the more flexible 2'-*endo* ribose conformation (103, 106, 143). This structural behavior originates from the nonplanar and nonaromatic nature of the D modification, where the double bond between *C*5-*C*6 of uridine is reduced to a single bond, shifting the atoms *C*5 and *C*6 on opposite sides of the *N*1, *C*2, *N*3, and *C*4 plane (149, 150). As D is no longer able to participate in stacking interactions with the neighboring aromatic residues, the modification increases the local flexibility of the D-loop. Moreover, D induces a 2'-*endo* conformation in the adjacent 5'-residue (74, 103, 151). The local flexibility of the D-loop may facilitate the interloop interaction of the conserved G_{18} and G_{19} residues with $Ψ_{55}$ and C_{56}, which are responsible for maintaining the structure of the elbow region (30, 103, 152). Because the lack of dihydrouridine in *E. coli* $tRNA^{Ser}_{GGA}$ is associated with a lower melting temperature, the flexibility of the D-loop must somehow contribute to tRNA stability (110). The NMR-based analysis of an RNA hairpin derived from *Schizosaccharomyces pombe* $tRNA_i^{Met}_{CAU}$ confirmed that the presence of D can indeed promote the formation of a stable RNA hairpin (152).

There are two additional uridine-based modifications that show a positive contribution to the structural stability of tRNAs. Thiolation of *C*4 at uridine 8 and 9 (s^4U) in the acceptor stem is conserved in bacteria and archaea but has not been reported in eukaryotes (92, 110, 153, 154). s^4U_8 is buried in the tRNA core and pairs with A_{14} of the D-loop. It has been suggested that s^4U is involved in tRNA stabilization, as lack of the modification decreased the melting temperature of *E. coli* $tRNA^{Ser}_{GGA}$ by 5 °C compared to the fully modified tRNA (110). The 3-(3-amino-3-carboxypropyl) uridine (acp^3U) modification prevents Watson-Crick base pairing and is located in the core region of tRNA (90, 151, 155, 156). acp^3U was initially detected in *E. coli* $tRNA^{Phe}_{GAA}$ and later on also found in several eukaryotic tRNAs (157–159). In *E. coli*, acp^3U is located at position 47 in the variable loop (151, 160, 161). It was shown that the presence of acp^3U_{47} in tRNAs of *E. coli* increases the melting temperature by 3 °C (160). However, in eukaryotes, acp^3U occurs in the D-loop at position 20 and 20a of several cytosolic tRNAs and at position 47 in plastid and mitochondrial-encoded tRNAs of various land plants (151, 160). Interestingly, $tRNA^{Lys}_{UUU}$ from *Trypanosoma brucei* has acp^3U at position 20 and a dihydrouridine derivative at position 47 (acp^3D). Despite its prevalence, the exact mechanistic and functional consequences of this acp^3D modification are not completely understood. It has been proposed that the presence of acp^3U in the variable loop might destabilize alternative tRNA conformations, as the acp^3 group blocks Watson-Crick pairing similar to m^1A^9 (160). Furthermore, it was suggested that acp^3U_{20a} might stabilize the local structure through Mg^{2+} coordination and that acp^3U_{47} could coordinate water or Mg^{2+} with the T-arm in a similar fashion to stabilize the local conformation (151, 160).

The various tRNA modifications can either happen as individual, independent events or as part of a complex modification circuitry that relies on a hierarchy of modifications (97, 98). These interdependencies between modification pathways are well described for the ASL, but recent work revealed the presence of a similar modification network also in the T-loop and tRNA core region (97, 98, 162, 163). In summary, the specific incorporation of tRNA modifications adds an additional layer of complexity that ensures the proper folding and structural stability of tRNAs. Foremost, the use of chemical modifications increases the number of RNA sequences that are able to fold into a functional tRNA and therefore the appearance of modification enzymes throughout evolution is directly correlated with the variation of tRNA sequences (164).

Recognition of the tRNA structure by modification enzymes and maturation factors

Although the shape of mature tRNAs must remain relatively rigid and stable to promote efficient translation of the ribosome, the structural characterization of precursor tRNAs that still need to undergo maturation suggests a very different scenario. In particular, analyses of tRNAs in complex with the proteins responsible for processing and modification provide insights into the dynamic nature of the tRNA structure itself, which could not be achieved by studying mature tRNAs alone or within the ribosome.

For several decades, X-ray crystallography and NMR have been the dominant methods for determining the structures of proteins bound to tRNAs. Numerous high-resolution structures of aminoacyl-tRNA-synthetases (type I aa-RS and type II aa-RS) in complex with their tRNA substrates have been reported and characteristic modes of tRNA recognition unveiled (Fig. 3*A*). Since 2010, eight crystal structures of tRNA-modifying enzymes bound to full-length tRNA have been reported, showing that these proteins use multiple approaches to recognize and bind substrate tRNAs. They can be either very specific to the target region or sense the global shape of tRNAs (Fig. 3*A*). *Thermus thermophilus* tRNA dihydrouridine synthase (*Tth*Dus) recognizes the elbow region of target tRNA and flips out the nucleotide at position 20 to present it to the catalytic active site (165). tRNA (cytosine (72)-C(5))-

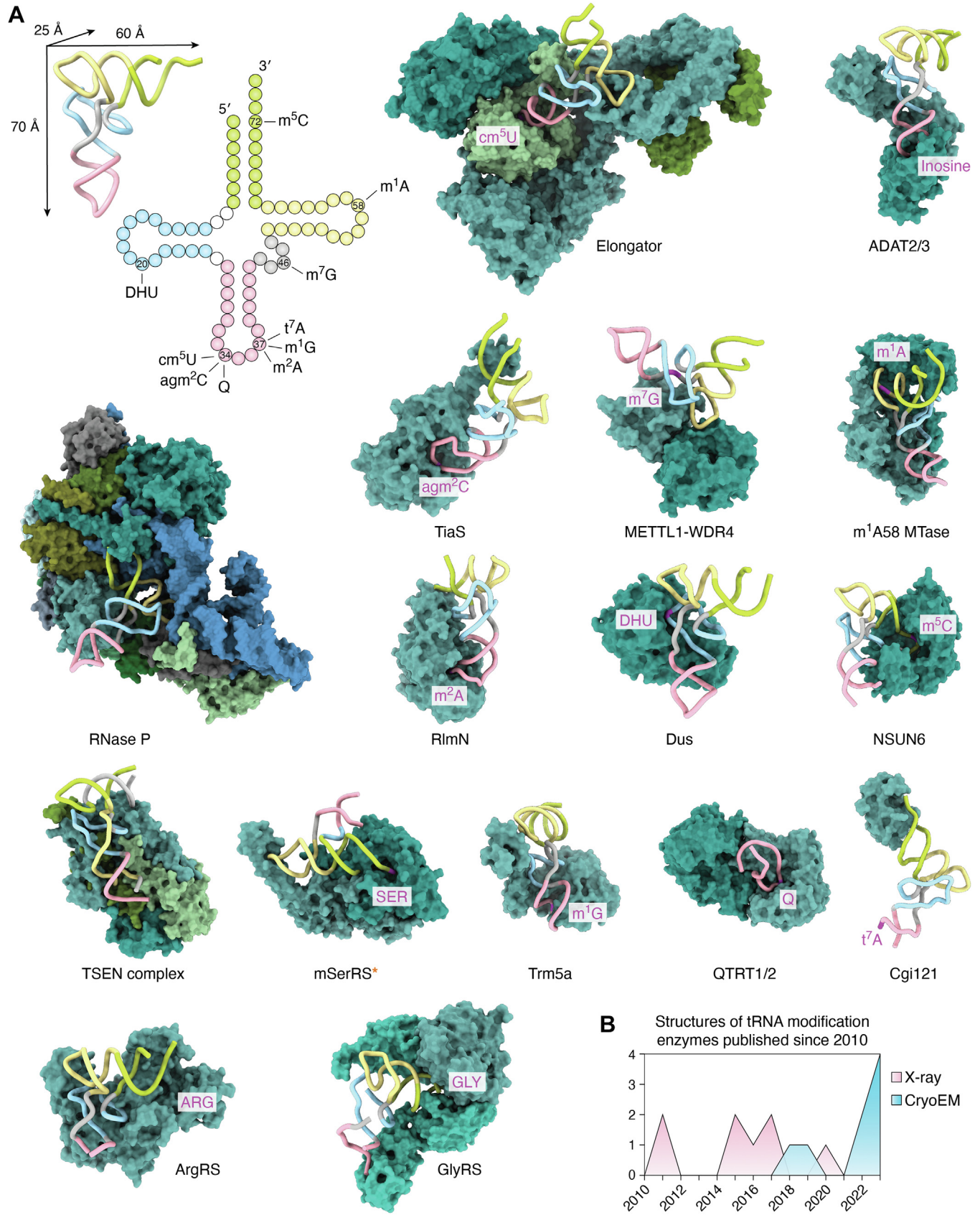

Figure 3. tRNA modification enzymes bind and recognize tRNAs using diverse strategies. *A*, gallery of available structures of tRNA modifying/processing enzymes solved with full-length tRNA (published since 2010). Precise modification sites are marked on the clover-leaf map of tRNA (*left upper* corner) and in the 3D structures (*magenta*). Elongator (PDB ID 8ASW), ADAT2/3 (PDB ID 8AW3), METTL1-WDR4 (PDB ID 8CTH), m^1A_{58} MTase (PDB ID 5CD1), mitochondrial seryl-tRNA synthetase (PDB ID 7U2B), Dus (PDB ID 3B0V), Ribonuclease P (PDB ID 6AHU), TiaS (PDB ID 3AMT), Trm5a (PDB ID 5WT3), NSUN6

methyltransferase (NSUN6), responsible for 5-methylcytosine modification in C_{72} of the AAS, recognizes the specific consensus sequence on the acceptor arm (166) but also senses the overall shape of target tRNAs by additional contacts. Similarly, the heterodimeric tRNA m^1A_{58} methyltransferase (m^1A_{58} MTase) buries the whole tRNA and breaks the interaction between D- and T-arms to gain access and to methylate the *N*1 position of A_{58} (167). Although a tetrameric form of m^1A_{58} MTase has been reported, it remains unclear if this represents a physiologically relevant oligomeric state of the complex.

Positions 34 and 37 on tRNAs, the modification hotspots in ASL, are modified with different moieties to guarantee a stringent decoding process. Despite these positions being in the same location on each tRNA, the mechanisms of binding and recognition for these positions differ dramatically. Such contextual recognition is essential for discrimination of nontarget from target tRNAs. For instance, $tRNA^{Ile}$-agm^2C synthetase (TiaS) binds to the acceptor arm and the ASL and catalyzes the modification on C_{34}. Contacts on the ASL stem are key substrate-specificity determinants of TiaS for $tRNA^{Ile}$ (168). tRNA methyltransferase (Trm5a) in *Pyrococcus abyssi* undergoes a conformational change to bind tRNAs *via* their elbow as well as ASL and executes the bifunctional methyltransfer at position G_{37} (169). The bacterial RNA methyltransferase (RlmN) modifies tRNA at A_{37}. It binds to the concave surface of tRNA, like most tRNA-modifying enzymes, suggesting that recognition of the entire tRNA molecule is key for this modification machinery. Its tRNA-binding mode resembles those of aminoacyl-tRNA-synthetases, which contact the 3′-end and D-arm of tRNA substrates (170). The "Kinase, endopeptidase and other protein of small size complex" (KEOPS) contacts the 3′-CCA tail of tRNA *via* its Cgi121 subunit, which is essential for t^6A_{37} modification (171). Details of how other subunits of the KEOPS complex orchestrate tRNA recognition is under investigation, but an initial tRNA–KEOPS complex model provides some insights into the potential reaction mechanism (172).

Because these tRNA-modifying enzymes act transiently and are highly dynamic, the chances of obtaining well-diffracting crystals are low thus scuttling structure determination. To overcome this problem, structural biologists have trimmed flexible regions of the proteins, crosslinked RNA to the complexes, or used point mutations to trap specific reaction intermediates. For instance, a crystal structure of heterodimeric human queuine tRNA-ribosyltransferase catalytic subunit 1 and 2 (QTRT1/2) crosslinked to a RNA stem-loop revealed details of substrate recognition and binding (173). These necessary compromises do raise concerns as to whether the obtained structures reflect the native architecture of the complexes. Foremost, the required quantities of homogenous tRNAs for macromolecular crystallography and NMR have complicated the determination of complexes with native tRNAs, reduced the variety of tRNA substrates used, and limited the number of structures of proteins in complex with full-length tRNA. For instance, out of the available repertoire of enzymes that modify tRNAs, the structures of only approximately 30% have been determined in complex with their tRNA target.

Recent developments in single-particle cryo-EM have boosted the field (Fig. 3*B*), allowing the structural characterization of enzymes in complex with tRNAs in their most natural conditions and requiring greatly reduced sample quantities. Moreover, advanced data analysis procedures allow delineation of different conformations and reaction states within the same sample, a feature that has the potential to provide a dynamic and more complete picture of the process of tRNA recognition and the underlying modification reaction itself. For example, the cryo-EM structure of the heterodimeric tRNA-specific adenosine deaminase 2/3 (ADAT2/3) complex bound to tRNA revealed that the anticodon loop, which harbors the modified nucleotide, is embedded in the catalytic site (174). The elbow region of the tRNA is recognized in a sequence-independent manner by distant regions of the protein located far from the catalytic core (174). Cryo-EM structures of the complex of methyltransferase 1-WD repeat–containing protein 4 (METTL1-WDR4) with a bound tRNA revealed that the noncatalytic subunit WDR4 interacts with the T-arm and is essential for the activity of METTL1, which further interacts with the elbow and modifies position 46 (175, 176).

Most of the known tRNA modification/processing enzymes exist as monomers or dimers and are usually relatively small (∼100 kDa) (62). One major exception is the 850-kDa eukaryotic Elongator complex, which is composed of two copies of its six individual subunits (*e.g.*, Elp1, Elp2, Elp3, Elp4, Elp5, and Elp6). The Elongator complex binds tRNA *via* two contact points (177). The Elp1 subunit contacts T- and D-arms (178), while the catalytic Elp3 subunit interacts with the ASL and carboxymethylates uridines in position 34 (179). Elongator recognizes the overall tRNA shape and can bind target as well as nontarget tRNAs with similar binding affinities *in vitro* (177). Another family of tRNA-processing enzymes that have recently been studied using single particle cryo-EM are well-known aminoacyl-tRNA synthetases. For instance, the cryo-EM structure of mitochondrial seryl-tRNA synthetase (mt-SerRS) ultimately shows how this protein specifically recognizes this rather unusual tRNA that lacks the D-arm. These enzymes recognize the radically altered T-arm topology, which leads to the loss of the canonical L-shape (180). Very recently, the structures of arginyl-tRNA synthetase (ArgRS) (181) and glycyl-tRNA

(PDB ID 5WWT), TSEN complex (PDB ID 7UXA/7ZRZ), RlmN (PDB ID 5HR6), QTRT1/2 (PDB ID 7NQ4), Cgi121 subunit of KEOPS (PDB ID 7KJT). All presented structures are cytoplasmic enzymes except for mitochondrial seryl-tRNA synthetase, which is marked by an *orange asterisk*. DusC from *Escherichia coli* (PDB ID 4YCP, 4YCO) is not shown as it is highly similar to *Tth*Dus (PDB ID 3B0V). The class I and class II aminoacyl tRNA synthetases are also included: arginyl-tRNA synthetase (ArgRS, PDB ID 5YYN) and glycyl-tRNA synthetase (GlyRS, PDB ID 7YSE). *B*, summary of the number of structures solved by different structural biology techniques together with full-length tRNA (2010–2022). KEOPS, Kinase, endopeptidase and other protein of small size complex.

synthetase (GlyRS) (182, 183) from different organisms have been determined in the presence of full-length tRNA.

Several cryo-EM studies of human RNase P bound to a mature tRNA reveal how a catalytic RNA aided by 10 protein subunits recognizes the acceptor-T stem stack for accurate pre-tRNA processing (184). Recent cryo-EM structures of human tRNA splicing endonuclease complex together with a pre-tRNA in precleavage and postcleavage states revealed how the multisubunit complex coordinates substrate recognition and the two-step cleavage reaction (185–187). Three subunits of tRNA splicing endonuclease interact with the T-arm, D-arm, and the anticodon stem, which acts as a ruler to correctly orient the 5′-splice site and 3′-splice site at the catalytic pocket.

tRNA modification and processing enzymes alter the structure of tRNA

The structural studies mentioned above also illustrate that the bound tRNAs undergo clearly observable conformational changes while binding to the enzymes and during the intermediate steps of the modification reactions. These conformational changes aim to properly recognize and position the tRNAs and expose the specific target site (or region) to the active site of the modifying enzyme. The movements can be observed in almost every region of tRNA, either as local movements proximal to the target nt or large scale global conformational changes (Fig. 4). For example, NSUN6 methylates C_{72} in $tRNA^{Cys}_{GCA}$ and $tRNA^{Thr}_{UGU}$ and distorts the conformation of the most distal 3' region (166). Likewise,

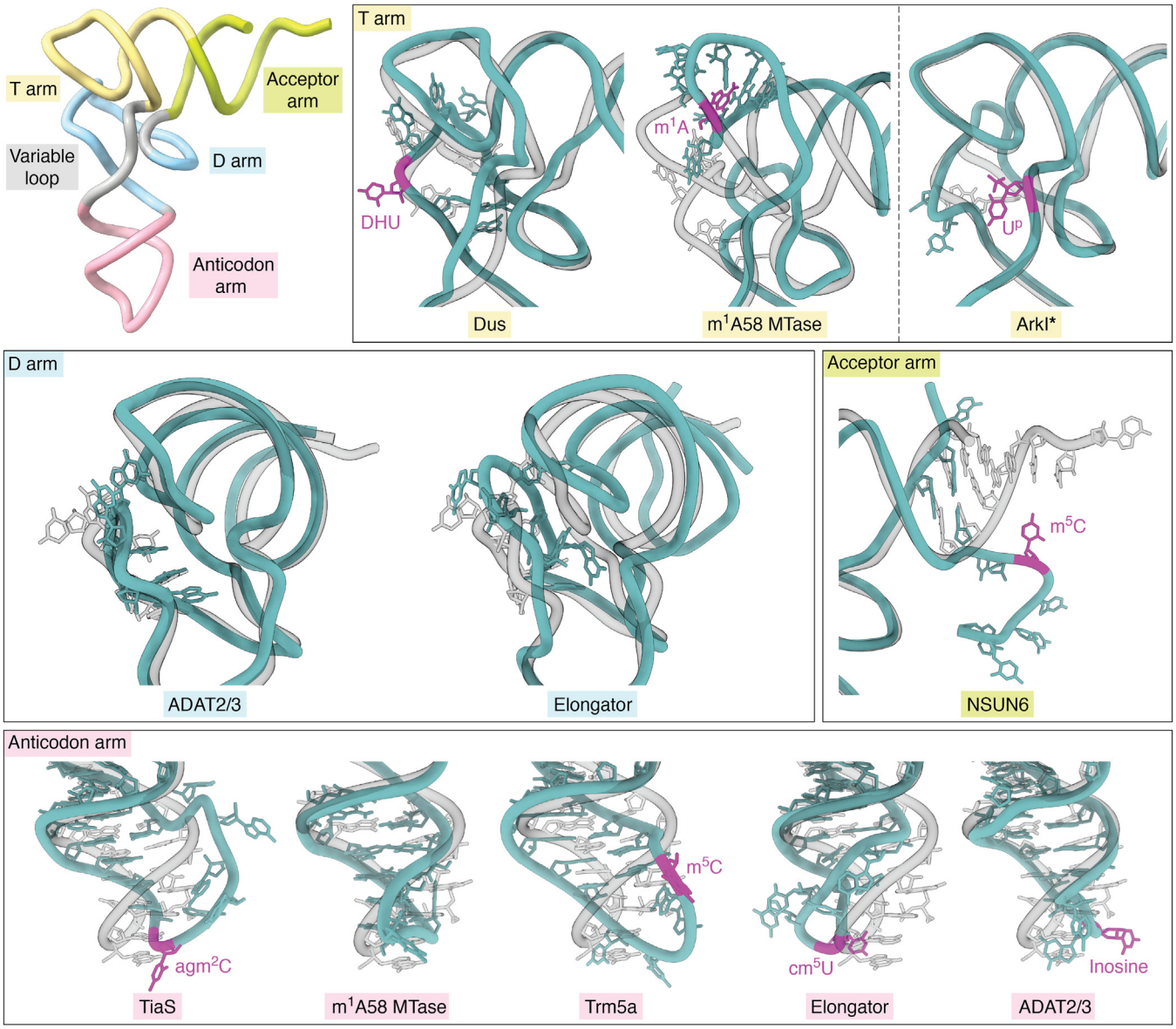

Figure 4. Modification enzymes influence tRNA structure in various regions. Yeast $tRNA^{Phe}_{GAA}$ (PDB ID 1EHZ) is aligned on each structure by the matchmaker tool in ChimeraX and shown transparently. Structures are sorted by the region affected structurally, and the names of the modifying enzymes are colored, accordingly. Modification sites are marked in *magenta*. Structures of full length-tRNAs are shown without their respective protein partners - Dus (PDB ID 3B0V), m^1A_{58} MTase (PDB ID 5CD1), Elongator (PDB ID 8ASW), ADAT2/3 (PDB ID 8AW3), TiaS (PDB ID 3AMT), Trm5a (PDB ID 5WT3), NSUN6 (PDB ID 5WWT). ArkI (PDB ID 7VNV) is a crystal structure of tRNA alone, modified by *Tk*ArkI.

changes in the elbow region of tRNA can be observed upon binding of tRNA-dihydrouridine synthase (165, 188).

In contrast, the binding of human m^1A_{58} MTase to tRNA not only changes the canonical shape of the elbow region (167) but also alters the shape of the ASL, which is distant from the modification site. Similarly, distant structural changes of the tRNA elbow were also reported in the *T. brucei* ADAT2/3 deaminase complex (174) and the yeast Elongator complex (178). A more drastic tRNA conformation change is observed in a complex with archaeosine tRNA-guanine transglycosylase, which forms a "λ form" of bound tRNA to allow the target site to be accessible to the enzyme (102). The phosphorylation of tRNA in position 47 by *Thermococcus kodakarensis* Arkl also influences the shape of the elbow region by restricting local backbone rotation (94) (Fig. 4). In this specific case, the described structural changes could be the consequence of the modification itself, as the observed differences are visible in the crystal structure of the phosphorylated tRNA in the absence of the modification enzyme. As these structures were obtained after trapping early reaction intermediates, these structural rearrangements are directly induced by the contacts between the tRNA and the protein complexes.

In all the cases presented above, the target nucleotides of the modification reaction were specifically flipped out from the canonical tRNA structure, facilitating access to the enzymatic active site. Although the three bases of the anticodon are already flipped out and accessible, this phenomenon is also visible in tRNA structures in complex with enzymes modifying residue 34 within the ASL (168, 174, 189) (Fig. 4). In all three mentioned cases, the conformation of the ASL is still further distorted, which may be necessary to discriminate between the other accessible bases and different tRNAs with similar anticodon sequences. In summary, the distortion of the tRNAs seems to be a common feature of almost all tRNA modification enzymes. Therefore, the respective proteins and protein complexes have evolved features that go beyond providing the enzymatic requirements for the respective modification reaction. They also guarantee the proper exposure of the specific target site. On the one hand, these additional conditions may have impeded modifications in certain positions on the tRNA. On the other hand, they may have supported the development of modification hotspots in certain domains (*e.g.*, ASL).

Unexpected appearance, function, and locations of tRNAs

In the previous sections, we summarized the specific three-dimensional features of tRNA molecules and described the fundamental determinants that influence their maturation and folding. In contrast to the conserved features, tRNAs sometimes do not obey their own rules and lack features that otherwise would appear crucial. Furthermore, some tRNAs are specifically cleaved and the obtained products can fulfill additional functions. Finally, as tRNAs are highly abundant, rigid building blocks present in all living cells, it is not surprising that they are also used in other cellular pathways and are even exploited by viruses and pathogens for their own benefit. In the following section, we summarize the most recently discovered and surprising examples of tRNAs, tRNA-like molecules, and tRNA-derived fragments.

Virus hijacking or mimicking host tRNAs

Viruses are known to hijack host molecules, such as rRNA and tRNAs, to enhance transcription, translation, and virion assembly (190). For instance, HIV type 1 retroviruses package host tRNAs during virion assembly and employ them as primers to initiate reverse transcription after infecting human cells. A recent study revealed a novel manner by which viruses recognize and utilize tRNAs from host cells. For instance, HIV type 1 virions are assembled by incorporation of multiple copies of the structural Gag protein, which selectively binds to several human tRNAs, including $tRNA^{Lys}_{CUU}$, $tRNA^{Lys}_{UUU}$, $tRNA^{Glu}_{CUC}$, $tRNA^{Glu}_{UUC}$, $tRNA^{Gly}_{GCC}$, $tRNA^{Gly}_{CCC}$, $tRNA^{Val}_{AAC}$, and $tRNA^{Val}_{CAC}$. The binding selectivity is achieved *via* the N-terminal matrix domain (MA) of Gag, which harbors four critical residues to track the characteristic tRNA elbow (191). The U-shape curvature and the invariant G_{19}-C_{56} pairing in the T-loop also contributes to tRNA recognition and selection. Of note, the binding of tRNAs occludes the strong basic surface area of MA, which prevents the interaction of Gag with membranes and thus prevents premature virion assembly. In stark contrast to the highly regulatory role of host tRNAs in the HIV-1 life cycle, human cytomegalovirus is also known to associate with human host RNA but the details remained unclear. Recently, Liu *et al.* used a combination of cryo-EM and deep RNA-seq to confirm the presence of tRNAs bound *via* pp150, a tegument protein forming a net-like density layer between the nucleocapsid and virion envelope (192). They identified at least six different cytosolic tRNA species, with $tRNA^{Glu}_{CUC}$ appearing to be the most abundant bound tRNA. Structurally, one tRNA molecule bridges three tegument pp150 proteins (Fig. 5*A*). The interactions are mediated *via* the phosphate backbone instead of specific base-stacking, explaining the low sequence-specificity. Surprisingly, this way of incorporating host tRNAs directly into the capsid seems to be unique for human cytomegalovirus because the structures of β-herpesviruses murine cytomegalovirus and human herpesvirus 6B capsids reveal no sign of tRNA association between their pp150 counterparts (192).

The term "tRNA-like structure" (TLS) refers to RNA motifs, which can fold into a tRNA fold. This type of a tRNA-mimicking motif was first discovered in the genome of positive-strand RNA Turnip yellow mosaic virus, and additional TLSs were identified later in other viruses and even mammals (193, 194). Apart from a predicted transcript with a sequence similar to tRNAs, several criteria need to be met to define a TLS. The potential TLS should (i) be able to fold into the full (or at least partial) shape of a tRNA (195), (ii) it should be able to interact with one or more tRNA-specific interactors (*e.g.*, aminoacyl-tRNA synthetases, RNase P, RNase Z, CCA-NTase, or eEF1A). Several TLS that fulfill these requirements reside in viral genomic RNAs, mRNAs, and noncoding RNAs. Employing tRNA mimicry is a relatively

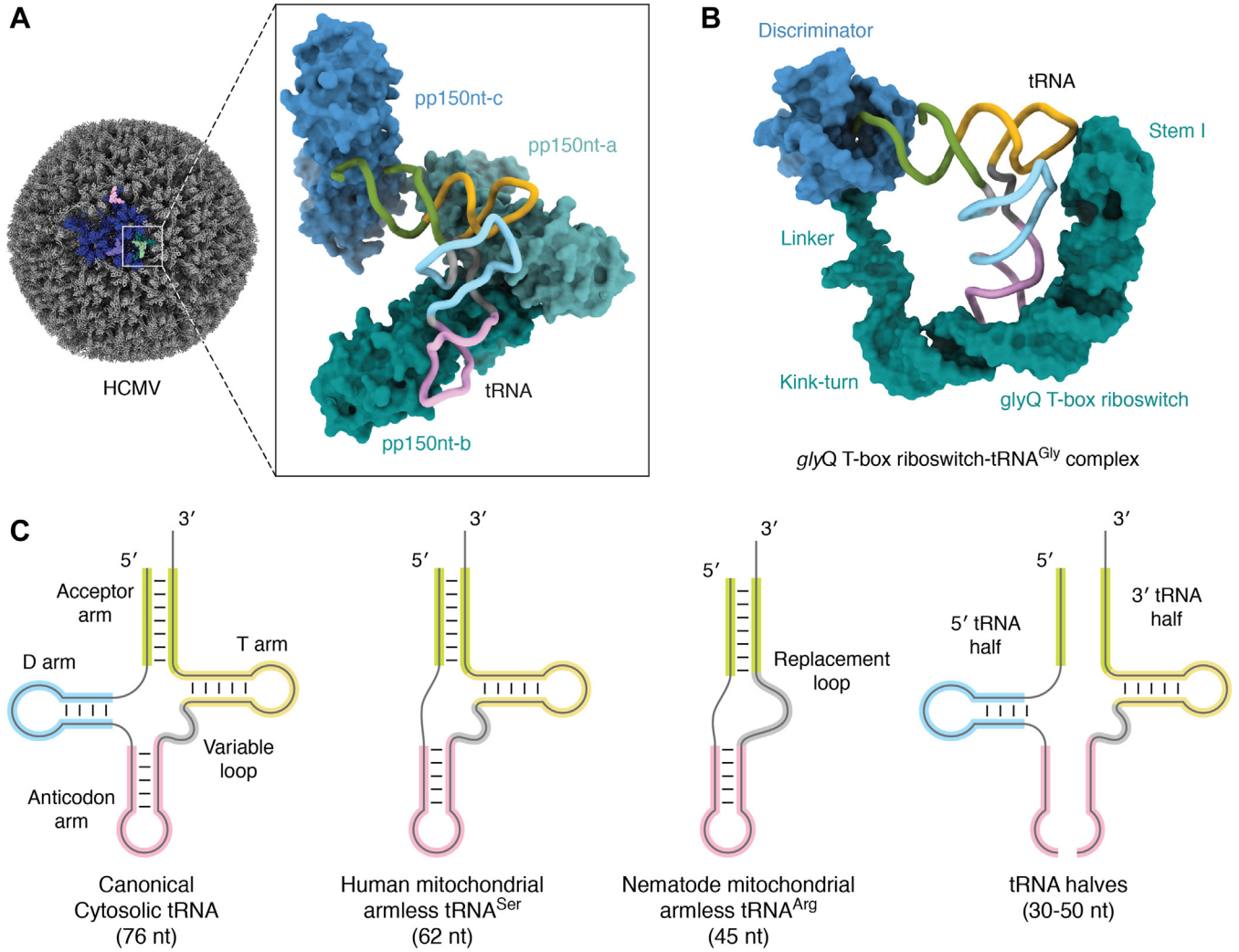

Figure 5. Examples of tRNAs with unexpected functions and atypical appearances. *A*, a cartoon representation of a cryo-EM structure of HCMV virion (PDB ID 5VKU) with tRNA bound to pp150 nt (inlet, PDB ID 7LJ3). The asymmetrical unit in the virion is colored in *blue* and the selected tRNAs are highlighted in *pink*, *purple*, and *green*. *B*, a cartoon representation of a cryo-EM structure of a full-length of *Bacillus subtilis glyQ* T-box-tRNA$^{Gly}_{GCC}$ complex (PDB ID 6POM). The tRNA is illustrated as spaghetti representation, while the binding partners are shown with surface representation. *C*, two-dimensional representation of various tRNA folds, including the canonical and truncated forms. HCMV, human cytomegalovirus.

simple strategy for viruses to hijack and to exploit the host's cellular inventory for its own purposes. For instance, the Hepatitis C virus harbors a tRNA-like domain in its internal ribosome entry sites to facilitate binding to the human 80S ribosome (196). A tRNA-like element has also been identified in the 5′ untranslated region of the HIV-1 genome proximal to the primer-binding site. This U-rich element mimics the anticodon loop of human tRNA$^{Lys}_{UUU}$ and competitively binds to lysyl-tRNA synthetase, thus increasing the availability of free tRNA$^{Lys}_{UUU}$, which serves as the primer for reverse transcription (197). As demonstrated in the crystal structure of Turnip yellow mosaic virus-TLS, the TLS folds into the characteristic L-shape, containing a pseudo-knotted acceptor stem (195). These TLSs can also be aminoacylated, like *bona fide* tRNAs. However, the selectivity of aminoacyl-tRNA synthetases limits aminoacylation of TLS to three amino acids, namely valine, histidine, and tyrosine. These various aminoacylated TLSs execute their function *via* different routes (198, 199). The TLS from Brome mosaic virus (BMV) has served as a model system to investigate the regulation of static and dynamic RNA structures for decades. For instance, the BMV TLS has been demonstrated to change conformation upon metal ion binding, which directly regulates viral replication (200). Recently, Bonilla *et al.* (201) presented the cryo-EM structures of the BMV TLS as well as the complex between TLS and tyrosyl-tRNA synthetase. Their work revealed how the BMV TLS undergoes conformational changes to interact with a host factor in a noncanonical fashion to achieve aminoacylation.

In stark contrast to the abundance of TLSs in viruses, only a limited number have been found in eukaryotic model organisms or humans (194). There are two known TLS in humans, namely mascRNA and *Men*β, which are the cleavage products derived from two long noncoding RNAs, namely metastasis-associated long adenocarcinoma transcript 1 (MALAT1) and Menβ (also known as NEAT1). Both TLSs are CCA-edited at their 3'-ends, but Menβ possesses an unstable acceptor stem

which prompts the CCA-NTase to add tandem CCA motifs and trigger degradation (202). Although mascRNA has a 3'-CCA, it is not aminoacylated. mascRNA has been linked to increased global protein synthesis and cell proliferation rates, as well as to several other cellular events, including antiviral and cardiovascular innate immunity regulation. A recent biochemical investigation demonstrated that mascRNA binds to glutaminyl-tRNA synthetase *via* its unique anticodon loop and upregulates glutaminyl-tRNA synthetase protein levels to promote protein translation (203). Although the aminoacyl-tRNA synthetase–enhanced protein translation is also observed in histidyl-tRNA synthetase (204), the details of this regulatory circuit remain elusive.

Y RNA-like A (YrlA) RNA represents a new class of tRNA mimicry, as it contains canonical tRNA motifs. YrlA RNA belongs to the family of Y RNAs, which are noncoding RNAs mostly found in bacteria and animal cells. The tRNA mimicry resembles the distinct tRNA L-shape (205), and these motifs are substrates of tRNA processing and modifying enzymes. The tRNA mimicry motif in Y RNA is believed to stabilize the structure and facilitate interaction with the Ro60 protein to regulate downstream cellular functions. Yet another kind of TLS is named nimtRNA for nuclear intronic mitochondrial-derived tRNAs. These nimtRNAs are transcribed from nuclear genomic DNA, which were originally derived from mitochondrial tRNA genes (206). These mitochondrial-tRNA look-alikes have been transferred and inserted into the human nuclear genome and are mainly found in the intronic regions of protein-coding or noncoding transcripts. Some of the sequences are identical to their mitochondrial predecessor, and others contain up to 25 mismatches while retaining the ability fold into the distinct tRNA structure (207). It has been shown that the presence of nimtRNAs in introns promotes pre-mRNA splicing and the tRNA-like motif seems crucial for the enhanced splicing efficiency.

tRNA sensing and metabolism

The T-box riboswitch is a regulatory noncoding RNA that binds to specifically uncharged tRNAs and thereby sense the availability of amino acids. This readout is used to attenuate downstream gene expression at the transcriptional or translational level (208). Over 23,000 T-box riboswitch domains are annotated according to the riboswitch database (209). These riboswitches are mainly found at the 5'-leader regions of certain mRNAs. Meanwhile, a smaller number of T-box riboswitches can be found mostly in *Actinobacteria*, where they control translation. In general, riboswitches act in a two-step sensory and regulatory mechanism. In the past decade, many crystal and cryo-EM structures of T-box riboswitches with the appropriate tRNA target have been reported, but most structures only contain parts of the riboswitch. Therefore, we lack a complete picture of how each motif of the riboswitch orchestrates the conformational changes upon tRNA binding (210). Recently, an intermediate resolution cryo-EM structure of the complete *Bacillus subtilis glyQ* T-box riboswitch, which belongs to the class that controls transcription, revealed the overall conformation during tRNA recognition (211) (Fig. 5*B*). The overall U-shape architecture of the riboswitch "clamps" the cognate $tRNA^{Gly}_{GCC}$ and the stem III, and discriminator domains sense the aminoacylation status (211). The regulatory domain can then switch between a terminator or antiterminator confirmation to govern the subsequent activation of transcription or translation (212). Overall, the recognition of cognate tRNA happens *via* the stem I domain of the riboswitch, which pairs the anticodon sequence of the tRNA with a "Specifier Sequence". A crystal structure of the full-length of *Mycobacterium tuberculosis ileS* T-box, which belongs to the class that controls translation, shows that it recognizes the cognate tRNA similar to the glyQ T-box but does not contact the tRNA elbow (213). Another crystal structure of stem I and stem II domains of a *Nocardia farcinica ileS* translational T-box riboswitch in complex with its cognate $tRNA^{Ile}_{GAU}$ reveals a different picture of how stem II reinforces the interaction of stem I and tRNA (214). In summary, the rigid structure of tRNAs is used by a variety of biosensors to determine the aminoacylation levels of tRNA, which is directly related to the metabolic state of the cell.

Glycosylated tRNAs

tRNA is heavily decorated with various chemical moieties (90), including the attachment of sugar groups. Queuosine (Q), a 7-deazaguanosine nucleoside, is obtained from gut bacteria and incorporated in the anticodon wobble position of cytosolic $tRNA^{Tyr}_{GUA}$, $tRNA^{His}_{GUG}$, $tRNA^{Asn}_{GUU}$, and $tRNA^{Asp}_{GUC}$ in humans (215). The Q-modified position 34 in $tRNA^{Tyr}_{GUA}$ and $tRNA^{Asp}_{GUC}$ is further "sugar coated". Unlike the polysaccharide conjugates on other noncoding RNAs, proteins, or lipid, $tRNA^{Tyr}_{GUA}$ and $tRNA^{Asp}_{GUC}$ carry a monosaccharide. Two glycosylated derivatives exist, namely galactose-Q (galQ)-$tRNA^{Tyr}_{GUA}$ and mannose-Q (manQ)-$tRNA^{Asp}_{GUC}$. A method has been developed using an acid-denaturing gel and northern blot to detect and quantify the presence galQ-$tRNA^{Tyr}_{GUA}$ and manQ-$tRNA^{Asp}_{GUC}$ (216). These glycosylated variants are found in all tested human organs without any tissue specificity, and the expression levels of all three modifications (galQ, manQ, and Q) seem to be correlated with age. These modified tRNAs are located in the cytosol and the nucleus. The enzyme responsible for this modification and the functional significance of this modification are yet to be identified. The chemical synthesis and the structure of galQ (217) and manQ (218) have been reported, while the biochemical pathways leading to them in living organisms still remains unknown. In addition to these known sugar modifications of $tRNA^{Tyr}_{GUA}$ and $tRNA^{Asp}_{GUC}$, a recent study employed a global labeling method and discovered that many tRNA species are attached to sialylated glycans in living cells (219). These so called "glyco-tRNAs" as well as other "glyco-RNAs" seem to be associated with membrane organelles and can also be detected on the cell surface. However, the modified sites on tRNAs and the detailed mechanism of RNA glycosylation are not known.

The atypical appearance of armless tRNAs

Despite the highly conserved L-shape structure of tRNA, there exists a group of structurally bizarre tRNAs (Fig. 5*C*) lacking D- and T-arms (220). They mostly exist in the mitochondria of nematodes, like *Caenorhabditis elegans* or *Ascaris suum*. Recently, it has also been found in the mitochondrial genome of arachnids (221). These structurally degenerate tRNAs are the consequences of the high mutations rates and genetic drift in the mitochondrial genome. Lack of either T-arm or D-arm (or both in extreme cases), as well as accumulation of weak base pairs and mismatches in stem regions, gives rise to the observed structural diversity (222–224). For instance, the smallest tRNA (with only 42 nt) has been identified in the mitochondria of *Dermatophagoides farina*, a mite. The predicted structure of two base-paired stems, connected by a variable bulge element, still resembles the dimensions and architecture of tRNAs (225). In the case of the T-armless tRNA, the canonical T-arm is replaced by a less structured 6- and 12-nt loop, named TV-replacement loop. Computational predictions show that some of these arm-less tRNAs retain the basic hairpin structure and adopt stable 3-D structures with "boomerang-like" shapes (224). Regardless of the missing parts, some of the miniaturized tRNAs have been proven to be functional, as they can be further edited by amino acid–specific aminoacyl-tRNA synthetases, CCA-NTase (226), and can be recognized by specific Elongator factor-Tu (EF-Tu) for mitochondrial protein translation (227). Of note, post-transcriptional modifications are also present on these arm-less tRNAs, including a methylation at position 9 (m^1A_9) (223). These modifications could stabilize mt-tRNA structure, enhance thermostability, and facilitate aminoacylation and translation. Correct aminoacylation of these arm-less tRNAs is crucial to ensure fidelity of mitochondrial translation. As the arm-less tRNA acts as an adapter (like the canonical tRNA), the mitochondrial EF-Tu1 and EF-Tu2 have undergone coevolutionary modulation to recognize features of these truncated tRNAs (228).

Mammals harbor mitochondrial tRNAs without D-arms, as exemplified by the mt-$tRNA^{Ser}_{GCU}$ iso-acceptors that show this deviated architecture (229). Similar to armless tRNAs from nematodes, mammalian mt-$tRNA^{Ser}_{GCU}$ also harbors RNA modifications (22), including three consecutive 5-methylcytosines (m^5C) at positions C_{47}, C_{49}, and C_{50}. A recent cryo-EM structure revealed the details of the armless mt-$tRNA^{Ser}_{GCU}$ in complex with human mitochondrial seryl-tRNA synthetase (180). Due to the lack of D arm, the mt-$tRNA^{Ser}_{GCU}$ loses its tRNA core domain and unexpectedly adopts an acute-angled "Y" shape. Furthermore, this drastically reshaped topology results in the loss of identity elements in mt-$tRNA^{Ser}_{GCU}$. As a consequence of this highly degenerated architecture, the human mitochondrial seryl-tRNA synthetase has also coevolved to bind to the specific acceptor stem of mt-$tRNA^{Ser}_{GCU}$ *via* its distinct helical arm and to charge the tRNA. Moreover, the stability of mt-$tRNA^{Ser}_{GCU}$ is sensitive to its tRNA charging status (230). The loss of mt-$tRNA^{Ser}_{GCU}$ is linked to retinal disease and class II mitochondrial seryl-tRNA-synthetase–related diseases (231).

Suppressor tRNAs

A subgroup of tRNAs exist as "suppressor tRNAs" in some species. These tRNAs can read through stop codons and nonsense mutations during translation (232, 233). They have been postulated to have resulted from mutations in the anti-codon sequence, which enabled pairing with stop codons and decoding nonsense mutations in mRNAs. Recently, Kachale *et al.* discovered a "reassignment" of an in-frame stop codon to $tRNA^{Trp}_{CCA}$ in a trypanosomatid, *Blastocrithidia nonstop*. A similar mechanism is also found in the ciliate *Condylostoma magnum*. Interestingly, $tRNA^{Trp}_{CCA}$ in both species harbors a shorter tRNA anticodon stem (from 5-bp to 4-bp). When a shorter anticodon stem version of $tRNA^{Trp}_{CCA}$ was engineered in yeast system, this specific tRNA indeed enhanced stop codon read-through (233). In principle, the simple engineering of the anticodon triplet of sense-coding tRNAs could transform them into suppressor tRNAs. However, only a few such mutant tRNAs have actually achieved high stop codon read-through activity and restored protein production (234). Various groups have taken different approaches (15, 235, 236) to understand what segments of tRNA are critical for suppression activity. Interestingly, redesigning the T-stem seems to be key strategy for suppressor tRNA to maintain a high decoding rate by strengthening the interaction with eEF1A.

The "+1-frameshift" (+1FS) suppressor tRNAs contain a single-nt insertion, which most often appears within the ASL (237–239). This extra nt generates a longer loop (8 nt), which differs from the canonical architecture. Nonetheless, the frameshift suppressor tRNA still decodes like a normal tRNA, as its anticodon is still defined by the universally conserved U_{33} and m^1G_{37} (240). The local ASL structure still undergoes distortion by disrupting the interaction between position 32 and 38 (239, 241, 242). A +1-frameshift takes place during translocation, which is mediated by +1FS suppressor tRNA, ribosome, mRNA, and elongation factor EF-G (241, 243, 244). These "slippery" tRNAs, which facilitate frameshifting of codon triplets, could be exploited biotechnologically (245).

tRNA in biotechnological and pharmaceutical applications

tRNA is not only important in fundamental regulation but also has been used in biotechnological and pharmaceutical applications. Ponchon and Dardel developed a system based on a camouflage strategy to fuse a target RNA with a tRNA scaffold (246). Due to the rigid and highly structured features of tRNA, the chimeric RNA was able to escape cellular RNase digestion. The target RNA can then be produced, purified, and released by RNase H treatment for downstream applications. Recently, Lee *et al.* (247) have taken the "tRNA-scaffold" approach and successfully determined the crystal structure of the ZIKA virus stem-loop A-tRNA to provide insights into the mechanism of stem-loop A–mediated RNA synthesis. As suppressor tRNAs naturally exist in a few species, the frameshift-suppressor tRNA or suppressor tRNA that decodes nonsense mutation have been employed in orthogonal translation systems (245). This strategy allows refactoring codons and incorporating noncanonical amino acids to expand the

genetic code for various designed functions. For instance, an engineered suppressor tRNA can be charged with the desired amino acid containing the glycan modification and this artificial product is incorporated into the target protein at the chosen position for further analyses (248). Moreover, decades ago, suppressor tRNAs have been proposed and engineered as a therapeutic tool to read through the premature codon termination. This method has been applied to several premature codon termination–related disease models, such as β-thalassemia (249) and cystic fibrosis transmembrane conductance regulator (234). The selected engineered tRNA indeed display promising effects on rescuing target protein production and restoring the responsible cellular function in cell and animal models (250, 251).

Future perspectives and directions

Despite the fact that tRNAs are highly structured and rigid RNA molecules, their dynamic and transient interactions with many processing factors and modification enzymes have complicated the structural analyses of the different maturation steps of tRNAs. Research on the dynamic structures of RNA domains has recently been changed fundamentally by the advent of high-resolution single particle cryo-EM (252). Recent examples (175, 176) have shown that cryo-EM facilitates the structural analyses of several different reaction intermediates without the need for identifying novel crystallization conditions for each individual conformation. We will most likely obtain whole galleries of structural snapshots for most tRNA modification reactions in the near future. Such an advance will fundamentally change our understanding of the sequential order of individual reaction steps and allow us to explore the dynamic transitions between them. Cryo-EM requires small amounts of sample, an attribute that will enable us to conduct structural studies on low-abundant RNAs isolated from endogenous sources or from sufficient quantities of *in vitro*–modified RNA samples. It is not only a new method to study previously known samples but it also allows us to rethink the list of RNA samples that can be visualized at high-resolution.

Recent advances in the field have essentially solved the fundamental problem of predicting three-dimensional structures of proteins from the primary amino acid sequence (253). The relatively small number of experimentally determined RNA and protein-RNA structures hinder the development of reliable models to predict the structure of these dynamic assemblies reliably *in silico*. Nonetheless, we are certain that the rapid advances in machine learning and molecular modeling will offer us significant support to understand the interaction between tRNAs and their cellular environment. Recently, an intermediate resolution cryo-EM structure of a DNA G-quadruplexes has demonstrated that we can reconstruct maps even for a 28-kDa biomolecule using electron microscopes (254). This advance suggests that RNAs with similar mass (*e.g.*, tRNAs, armless tRNAs, Y RNAs, or tRNA-like molecule) can also be analyzed by cryo-EM. It remains to be shown whether one can obtain near-atomic resolution structures of RNAs that are more dynamic than proteins. As certain RNA modifications are known to increase the stability/rigidity of RNAs, these modifications may be exploited to achieve higher resolution structures.

Apart from studies on tRNA and tRNA-like molecules, numerous functional studies have identified subpopulations of small noncoding RNAs that are derived from tRNA, called tRNA halves or tRNA-derived fragments (Fig. 5*C*). These tRNA derivatives, either as separated tRNA halves or as a nicked tRNA complex, were reported to be involved in a plethora of cellular functions and pathways (255–258).

As mentioned above, it still remains unclear if and how individual tRNA modification cascades are coupled or even depend on each other (97, 98, 162, 163). The first time-resolved NMR studies have tried to dissect the hierarchy of tRNA decoration and highlight the exciting complementary opportunities to record multiple modifications steps in parallel (162, 259). As tRNA modifications can directly influence the folding of tRNAs, the efficiency of the underlying modification reactions might provide another route to control cellular translation. As some of the modification cascades directly rely on basic metabolic pathways (260–262), tRNA-related processes might represent molecular switches between the metabolic state and the regulation of protein synthesis in a cell. Therefore, we need to fully understand tRNA processing and modification pathways at the cellular and organismal level in the future.

A major question that needs to be addressed soon is the actual role of the processing and modification enzymes for the functionality of tRNAs. We lack a fundamental mechanistic understanding of whether the tRNA-interacting proteins can contribute more than "just" attaching chemical groups or if they also act as molecular chaperones or regulators. Here, the biophysical and structural analyses of tRNAs before and after a specific modification reaction might provide direct insights. Furthermore, it remains to be shown whether tRNA splicing and processing activate or respond to specific tRNA modifications. Finally, modified nt of tRNAs, mRNAs, and ribosomal RNA are proximal to one another during ribosomal decoding. We need to understand whether these molecules and their modifications communicate with one another to reveal yet another regulatory layer of gene expression.

Finally, tRNA-based technologies seem to have a very bright future in the field of personalized biomedicine, especially if suppressor tRNAs break the current limitations of highly selective aminoacyl-tRNA synthetases. Here, natural variations of tRNAs and translation systems can and should inspire us to develop novel tRNA-based tools and technologies that could enable us to control, correct, or restore cellular protein synthesis.

Acknowledgments—We would like to thank all members of the Glatt lab for insightful discussion during the preparation of this manuscript and Jonathan G. Heddle for additional comments. We used ChimeraX for illustrating protein-tRNA structures and ChemSketch for depicting chemical modifications. Due to the vast number of published studies in the field, we were not able to

refer to all the available publications. Therefore, we would apologize to all researchers in the community who were not directly cited or acknowledged.

Author contributions—A. B., A. H., I. K., M. W., L. K., T.-Y. L., and S. G. writing–original draft; A. B., A. H., I. K., M. W., L. K., T.-Y. L., and S. G. visualization; T.-Y. L. and S. G. conceptualization; A. B., A. H., I. K., M. W., L. K., T.-Y. L., and S. G. investigation.

Funding and additional information—This work was supported by the European Research Council (ERC) under the European Union's Horizon 2020 research and innovation program (grant agreement No 101001394 to S. G.).

Conflict of interest—The authors declare that they have no conflicts of interest with the contents of this article.

Abbreviations—The abbreviations used are: 2'-OMe, 2'-OH moiety; AAS, amino acid accepting stem; acp, aminocarboxypropylation; ASL, anticodon stem loop; BMV, Brome mosaic virus; EF-Tu, Elongator factor-Tu; KEOPS, Kinase, endopeptidase and other protein of small size complex; nimtRNA, nuclear intronic mitochondrial-derived tRNA; TLS, tRNA-like structure.

References

1. Crick, F. H. (1958) On protein synthesis. *Symp. Soc. Exp. Biol.* **12**, 138–163
2. Roeder, R. G., and Rutter, W. J. (1969) Multiple forms of DNA-dependent RNA polymerase in eukaryotic organisms. *Nature* **224**, 234–237
3. Weinmann, R., Raskas, H. J., and Roeder, R. G. (1974) Role of DNA dependent RNA polymerases II and III in transcription of the adenovirus genome late in productive infection. *Proc. Natl. Acad. Sci. U. S. A.* **71**, 3426–3430
4. Chan, P. P., and Lowe, T. M. (2016) GtRNAdb 2.0: an expanded database of transfer RNA genes identified in complete and draft genomes. *Nucleic Acids Res.* **44**, D184–D189
5. Baranov, P. V., Gesteland, R. F., and Atkins, J. F. (2002) Recoding: translational bifurcations in gene expression. *Gene* **286**, 187–201
6. Lai, L. B., Lai, S. M., Szymanski, E. S., Kapur, M., Choi, E. K., Al-Hashimi, H. M., *et al.* (2022) Structural basis for impaired 50 processing of a mutant tRNA associated with defects in neuronal homeostasis. *Proc. Natl. Acad. Sci. U. S. A.* **119**, e2119529119
7. Abbott, J. A., Francklyn, C. S., and Robey-Bond, S. M. (2014) Transfer RNA and human disease. *Front. Genet.* **5**, 158
8. Goodarzi, H., Nguyen, H. C. B., Zhang, S., Dill, B. D., Molina, H., and Tavazoie, S. F. (2016) Modulated expression of specific tRNAs drives gene expression and cancer progression. *Cell* **165**, 1416–1427
9. Torres, A. G., Batlle, E., and Ribas de Pouplana, L. (2014) Role of tRNA modifications in human diseases. *Trends Mol. Med.* **20**, 306–314
10. Schaffer, A. E., Pinkard, O., and Coller, J. M. (2019) tRNA metabolism and neurodevelopmental disorders. *Annu. Rev. Genomics Hum. Genet.* **20**, 359–387
11. Kirchner, S., and Ignatova, Z. (2015) Emerging roles of tRNA in adaptive translation, signalling dynamics and disease. *Nat. Rev. Genet.* **16**, 98–112
12. Hawer, H., Hammermeister, A., Ravichandran, K. E., Glatt, S., Schaffrath, R., and Klassen, R. (2019) Roles of elongator dependent tRNA modification pathways in neurodegeneration and cancer. *Genes (Basel)* **10**, 1–23
13. Gaik, M., Kojic, M., Stegeman, M. R., Öncü-Öner, T., Kościelniak, A., Jones, A., *et al.* (2022) Functional divergence of the two elongator subcomplexes during neurodevelopment. *EMBO Mol. Med.* **14**, e15608
14. Kojic, M., and Wainwright, B. (2016) The many faces of elongator in neurodevelopment and disease. *Front. Mol. Neurosci.* **9**, 115
15. Albers, S., Beckert, B., Matthies, M. C., Mandava, C. S., Schuster, R., Seuring, C., *et al.* (2021) Repurposing tRNAs for nonsense suppression. *Nat. Commun.* **12**, 1–10
16. Sharp, S. J., Schaack, J., Cooley, L., Burke, D. J., and Soil, D. (1985) Structure and transcription of eukaryotic tRNA gene. *Crit. Rev. Biochem. Mol. Biol.* **19**, 107–144
17. Holley, R. W., Apgar, J., Everett, G. A., Madison, J. T., Marquisee, M., Merrill, S. H., *et al.* (1965) Structure of a ribonucleic acid. *Science* **147**, 1462–1465
18. Giegé, R., Jühling, F., Pütz, J., Stadler, P., Sauter, C., and Florentz, C. (2012) Structure of transfer RNAs: similarity and variability. *Wiley Interdiscip. Rev. RNA* **3**, 37–61
19. Betat, H., Rammelt, C., and Mörl, M. (2010) tRNA nucleotidyltransferases: ancient catalysts with an unusual mechanism of polymerization. *Cell. Mol. Life Sci.* **67**, 1447–1463
20. Sprinzl, M., and Cramer, F. (1979) The -C-C-A end of tRNA and its role in protein biosynthesis. *Prog. Nucleic Acid Res. Mol. Biol.* **22**, 1–69
21. Hamashima, K., Tomita, M., and Kanai, A. (2016) Expansion of non-canonical V-arm-containing tRNAs in eukaryotes. *Mol. Biol. Evol.* **33**, 530–540
22. Suzuki, T., Yashiro, Y., Kikuchi, I., Ishigami, Y., Saito, H., Matsuzawa, I., *et al.* (2020) Complete chemical structures of human mitochondrial tRNAs. *Nat. Commun.* **11**, 4269
23. Pütz, J., Dupuis, B., Sissler, M., and Florentz, C. (2007) Mamit-tRNA, a database of mammalian mitochondrial tRNA primary and secondary structures. *RNA* **13**, 1184–1190
24. Hafez, M., Burger, G., Steinberg, S. V., and Lang, F. (2013) A second eukaryotic group with mitochondrion-encoded tmRNA. *RNA Biol.* **10**, 1117–1124
25. Hamashima, K., Fujishima, K., Masuda, T., Sugahara, J., Tomita, M., and Kanai, A. (2012) Nematode-specific tRNAs that decode an alternative genetic code for leucine. *Nucleic Acids Res.* **40**, 3653–3662
26. Jühling, F., Pütz, J., Florentz, C., and Stadler, P. F. (2012) Armless mitochondrial tRNAs in Enoplea (Nematoda). *RNA Biol.* **9**, 1161–1166
27. Lorenz, C., Lünse, C. E., and Mörl, M. (2017) tRNA modifications: impact on structure and thermal adaptation. *Biomolecules* **7**, 35
28. Madore, E., Florentz, C., Giege, R., and Lapointe, J. (1999) Magnesium-dependent alternative foldings of active and inactive Escherichia coli tRNAGlu revealed by chemical probing. *Nucleic Acids Res.* **27**, 3583–3588
29. Steinberg, S., Leclerc, F., and Cedergren, R. (1997) Structural rules and conformational compensations in the tRNA L-form 1 1Edited by D. E. Draper. *J. Mol. Biol.* **266**, 269–282
30. Zhang, J., and Ferré-D'Amaré, A. (2016) The tRNA elbow in structure, recognition and evolution. *Life* **6**, 3
31. Robertus, J. D., Ladner, J. E., Finch, J. T., Rhodes, D., Brown, R. S., Clark, B. F. C., *et al.* (1974) Structure of yeast phenylalanine tRNA at 3 Å resolution. *Nature* **250**, 546–551
32. Kim, S. H., Suddath, F. L., Quigley, G. J., McPherson, A., Sussman, J. L., Wang, A. H. J., *et al.* (1974) Three-dimensional tertiary structure of yeast phenylalanine transfer RNA. *Science* **185**, 435–440
33. Suddath, F. L., Quigley, G. J., McPherson, A., Sneden, D., Kim, J. J., Kim, S. H., *et al.* (1974) Three-dimensional structure of yeast phenylalanine transfer RNA at 3. 0Å resolution. *Nature* **248**, 20–24
34. Jovine, L., Djordjevic, S., and Rhodes, D. (2000) The crystal structure of yeast phenylalanine tRNA at 2.0 Å resolution: cleavage by Mg2+ in 15-year old crystals. *J. Mol. Biol.* **301**, 401–414
35. Moras, D., Comarmond, M. B., Fischer, J., Weiss, R., Thierry, J. C., Ebel, J. P., *et al.* (1980) Crystal structure of yeast tRNAAsp. *Nature* **288**, 669–674
36. Westhof, E., Dumas, P., and Moras, D. (1985) Crystallographic refinement of yeast aspartic acid transfer RNA. *J. Mol. Biol.* **184**, 119–145
37. Woo, N. H., Roe, B. A., and Rich, A. (1980) Three-dimensional structure of Escherichia coli initiator tRNAfMet. *Nature* **286**, 346–351
38. Basavappa, R., and Sigler, P. B. (1991) The 3 A crystal structure of yeast initiator tRNA: functional implications in initiator/elongator discrimination. *EMBO J.* **10**, 3105–3111

39. Bénas, P., Bec, G., Keith, G., Marquet, R., Ehresmann, C., Ehresmann, B., *et al.* (2000) The crystal structure of HIV reverse-transcription primer tRNA(Lys,3) shows a canonical anticodon loop. *RNA* **6**, 1347–1355
40. Väre, V., Eruysal, E., Narendran, A., Sarachan, K., and Agris, P. (2017) Chemical and conformational diversity of modified nucleosides affects tRNA structure and function. *Biomolecules* **7**, 29
41. Crothers, D. M., Seno, T., and Söll, G. (1972) Is there a discriminator site in transfer RNA? *Proc. Natl. Acad. Sci. U. S. A.* **69**, 3063–3067
42. Cooley, L., Appel, B., and Söll, D. (1982) Post-transcriptional nucleotide addition is responsible for the formation of the 5′ terminus of histidine tRNA. *Proc. Natl. Acad. Sci. U. S. A.* **79**, 6475–6479
43. Giege, R., Sissler, M., and Florentz, C. (1998) Universal rules and idiosyncratic features in tRNA identity. *Nucleic Acids Res.* **26**, 5017–5035
44. Giegé, R., and Eriani, G. (2023) The tRNA identity landscape for aminoacylation and beyond. *Nucleic Acids Res.* **51**, 1528–1570
45. Frank, D. N., and Pace, N. R. (1998) Ribonuclease P: unity and diversity in a tRNA processing ribozyme. *Annu. Rev. Biochem.* **67**, 153–180
46. Kerkhofs, K., Garg, J., Fafard-Couture, É., Abou Elela, S., Scott, M. S., Pearlman, R. E., *et al.* (2022) Altered tRNA processing is linked to a distinct and unusual La protein in Tetrahymena thermophila. *Nat. Commun.* **13**, 1–17
47. Deutscher, M. P. (2006) Degradation of RNA in bacteria: comparison of mRNA and stable RNA. *Nucleic Acids Res.* **34**, 659–666
48. Li, Z., and Deutscher, M. P. (1996) Maturation pathways for E. coli tRNA precursors: a random multienzyme process *in vivo*. *Cell* **86**, 503–512
49. Ezraty, B., Dahlgren, B., and Deutscher, M. P. (2005) The RNase Z homologue encoded by Escherichia coli elaC gene is RNase BN. *J. Biol. Chem.* **280**, 16542–16545
50. Pellegrini, O. (2003) Endonucleolytic processing of CCA-less tRNA precursors by RNase Z in Bacillus subtilis. *EMBO J.* **22**, 4534–4543
51. Deutscher, M. P. (1982) 7 tRNA nucleotidyltransferase. *Enzymes* **15**, 183–215
52. Moazed, D., and Noller, H. F. (1991) Sites of interaction of the CCA end of peptidyl-tRNA with 23S rRNA. *Proc. Natl. Acad. Sci. U. S. A.* **88**, 3725–3728
53. Korostelev, A., Trakhanov, S., Laurberg, M., and Noller, H. F. (2006) Crystal structure of a 70S ribosome-tRNA complex reveals functional interactions and rearrangements. *Cell* **126**, 1065–1077
54. Hou, Y.-M. (1993) The tertiary structure of tRNA and the development of the genetic code. *Trends Biochem. Sci.* **18**, 362–364
55. Graifer, D., and Karpova, G. (2015) Interaction of tRNA with eukaryotic ribosome. *Int. J. Mol. Sci.* **16**, 7173–7194
56. Sigler, P. B. (1975) An analysis of the structure of tRNA. *Annu. Rev. Biophys. Bioeng.* **4**, 477–527
57. Sprinzl, M. (1998) Compilation of tRNA sequences and sequences of tRNA genes. *Nucleic Acids Res.* **26**, 148–153
58. Giegé, R., and Frugier, M. (2000-2013) Transfer RNA structure and identity. In: *Madame Curie Bioscience Database [Internet]*. Bioscience, Austin (TX): Landes
59. Chiba, S., Itoh, Y., Sekine, S., and Yokoyama, S. (2010) Structural basis for the major role of O-phosphoseryl-tRNA kinase in the UGA-specific encoding of selenocysteine. *Mol. Cell* **39**, 410–420
60. Hilal, T., Killam, B. Y., Grozdanović, M., Dobosz-Bartoszek, M., Loerke, J., Bürger, J., *et al.* (2022) Structure of the mammalian ribosome as it decodes the selenocysteine UGA codon. *Science* **376**, 1338–1343
61. Hao, B., Gong, W., Ferguson, T. K., James, C. M., Krzycki, J. A., and Chan, M. K. (2002) A new UAG-encoded residue in the structure of a methanogen methyltransferase. *Science* **296**, 1462–1466
62. Krutyhołowa, R., Zakrzewski, K., and Glatt, S. (2019) Charging the code — tRNA modification complexes. *Curr. Opin. Struct. Biol.* **55**, 138–146
63. Amann, S. J., Keihsler, D., Bodrug, T., Brown, N. G., and Haselbach, D. (2023) Frozen in time: analyzing molecular dynamics with time-resolved cryo-EM. *Structure* **31**, 4–19
64. Loveland, A. B., Demo, G., and Korostelev, A. A. (2020) Cryo-EM of elongating ribosome with EF-Tu•GTP elucidates tRNA proofreading. *Nature* **584**, 640–645
65. Carbone, C. E., Loveland, A. B., Gamper, H. B., Hou, Y. M., Demo, G., and Korostelev, A. A. (2021) Time-resolved cryo-EM visualizes ribosomal translocation with EF-G and GTP. *Nat. Commun.* **12**, 7236
66. Giegé, R., Frugier, M., and Rudinger, J. (1998) tRNA mimics. *Curr. Opin. Struct. Biol.* **8**, 286–293
67. Butcher, S. E., and Jan, E. (2016) tRNA-mimicry in IRES-mediated translation and recoding. *RNA Biol.* **13**, 1068–1074
68. Francisco-Velilla, R., Embarc-Buh, A., Abellan, S., and Martinez-Salas, E. (2022) Picornavirus translation strategies. *FEBS Open Bio* **12**, 1125–1141
69. Trachman, R. J., Passalacqua, L. F. M., and Ferré-D'Amaré, A. R. (2022) The bacterial yjdF riboswitch regulates translation through its tRNA-like fold. *J. Biol. Chem.* **298**, 101934
70. Czworkowski, J., Wang, J., Steitz, T. A., and Moore, P. B. (1994) The crystal structure of elongation factor G complexed with GDP, at 2.7 A resolution. *EMBO J.* **13**, 3661–3668
71. Nyborg, J., Nissen, P., Kjeldgaard, M., Thirup, S., Polekhina, G., Clark, B. F. C., *et al.* (1996) Structure of the ternary complex of EF-Tu: macromolecular mimicry in translation. *Trends Biochem. Sci.* **21**, 81–82
72. Selmer, M., Al-Karadaghi, S., Hirokawa, G., Kaji, A., and Liljas, A. (1999) Crystal structure of Thermotoga maritima ribosome recycling factor: a tRNA mimic. *Science* **286**, 2349–2352
73. Jørgensen, R., Ortiz, P. A., Carr-Schmid, A., Nissen, P., Kinzy, T. G., and Andersen, G. R. (2003) Two crystal structures demonstrate large conformational changes in the eukaryotic ribosomal translocase. *Nat. Struct. Mol. Biol.* **10**, 379–385
74. Shi, H., and Moore, P. B. (2000) The crystal structure of yeast phenylalanine tRNA at 1.93 Å resolution: a classic structure revisited. *RNA* **6**, 1091–1105
75. Byrne, R. T., Konevega, A. L., Rodnina, M. V., and Antson, A. A. (2010) The crystal structure of unmodified tRNAPhe from Escherichia coli. *Nucleic Acids Res.* **38**, 4154–4162
76. Kimura, S., Suzuki, T., Chen, M., Kato, K., Yu, J., Nakamura, A., *et al.* (2016) Template-dependent nucleotide addition in the reverse (3′-5′) direction by Thg1-like protein. *Sci. Adv.* **2**, e1501397
77. Bourgeois, G., Seguin, J., Babin, M., Gondry, M., Mechulam, Y., and Schmitt, E. (2020) Structural basis of the interaction between cyclodipeptide synthases and aminoacylated tRNA substrates. *RNA* **26**, 1589–1602
78. Harrington, K. M., Nazarenko, I. A., Uhlenbeck, O. C., Dix, D. B., and Thompson, R. C. (1993) *In vitro* analysis of translational rate and accuracy with an unmodified tRNA. *Biochemistry* **32**, 7617–7622
79. Perret, V., Garcia, A., Puglisi, J., Grosjean, H., Ebel, J. P., Florentz, C., *et al.* (1990) Conformation in solution of yeast tRNAAsp transcripts deprived of modified nucleotides. *Biochimie* **72**, 735–743
80. Saks, M. E., Sampson, J. R., and Abelson, J. N. (1994) The transfer RNA identity problem: a search for rules. *Science* **263**, 191–197
81. Sampson, J. R., and Uhlenbeck, O. C. (1988) Biochemical and physical characterization of an unmodified yeast phenylalanine transfer RNA transcribed *in vitro*. *Proc. Natl. Acad. Sci. U. S. A.* **85**, 1033–1037
82. Bhaskaran, H., Rodriguez-Hernandez, A., and Perona, J. J. (2012) Kinetics of tRNA folding monitored by aminoacylation. *RNA* **18**, 569–580
83. Derrick, W. B., and Horowitz, J. (1993) Probing structural differences between native and *in vitro* transcribed Escherichia coli valine transfer RNA: evidence for stable base modification-dependent conformers. *Nucleic Acids Res.* **21**, 4948–4953
84. Dewe, J. M., Whipple, J. M., Chernyakov, I., Jaramillo, L. N., and Phizicky, E. M. (2012) The yeast rapid tRNA decay pathway competes with elongation factor 1A for substrate tRNAs and acts on tRNAs lacking one or more of several modifications. *RNA* **18**, 1886–1896
85. Helm, M., Brulé, H., Degoul, F., Cepanec, C., Leroux, J. P., Giegé, R., *et al.* (1998) The presence of modified nucleotides is required for cloverleaf folding of a human mitochondrial tRNA. *Nucleic Acids Res.* **26**, 1636–1643
86. Phizicky, E. M., and Alfonzo, J. D. (2010) Do all modifications benefit all tRNAs? *FEBS Lett.* **584**, 265–271
87. Vermeulen, A., McCallum, S. A., and Pardi, A. (2005) Comparison of the global structure and dynamics of native and unmodified tRNAval. *Biochemistry* **44**, 6024–6033

88. Maglott, E. J., Deo, S. S., Przykorska, A., and Glick, G. D. (1998) Conformational transitions of an unmodified tRNA: implications for RNA folding. *Biochemistry* **37**, 16349–16359
89. Serebrov, V., Vassilenko, K., Kholod, N., Gross, H. J., and Kisselev, L. (1998) Mg2+ binding and structural stability of mature and *in vitro* synthesized unmodified Escherichia coli tRNA(Phe). *Nucleic Acids Res.* **26**, 2723–2728
90. Boccaletto, P., Stefaniak, F., Ray, A., Cappannini, A., Mukherjee, S., Zbieta Purta, E., *et al.* (2021) MODOMICS: a database of RNA modification pathways. 2021 update. *Nucleic Acids Res.* **50**, D231–D235
91. Jackman, J. E., and Alfonzo, J. D. (2013) Transfer RNA modifications: nature's combinatorial chemistry playground. *Wiley Interdiscip. Rev. RNA* **4**, 35–48
92. Jühling, F., Mörl, M., Hartmann, R. K., Sprinzl, M., Stadler, P. F., and Pütz, J. (2009) tRNAdb 2009: compilation of tRNA sequences and tRNA genes. *Nucleic Acids Res.* **37**, D159–D162
93. Motorin, Y., and Helm, M. (2010) tRNA stabilization by modified nucleotides. *Biochemistry* **49**, 4934–4944
94. Ohira, T., Minowa, K., Sugiyama, K., Yamashita, S., Sakaguchi, Y., Miyauchi, K., *et al.* (2022) Reversible RNA phosphorylation stabilizes tRNA for cellular thermotolerance. *Nature* **605**, 372–379
95. Suzuki, T. (2021) The expanding world of tRNA modifications and their disease relevance. *Nat. Rev. Mol. Cell Biol.* **22**, 375–392
96. Schaffrath, R., and Leidel, S. A. (2017) Wobble uridine modifications–a reason to live, a reason to die?! *RNA Biol.* **14**, 1209–1222
97. Han, L., and Phizicky, E. M. (2018) A rationale for tRNA modification circuits in the anticodon loop. *RNA* **24**, 1277–1284
98. Sokolowski, M., Klassen, R., Bruch, A., Schaffrath, R., and Glatt, S. (2018) Cooperativity between different tRNA modifications and their modification pathways. *Biochim. Biophys. Acta* **1861**, 409–418
99. Duechler, M., Leszczyńska, G., Sochacka, E., and Nawrot, B. (2016) Nucleoside modifications in the regulation of gene expression: focus on tRNA. *Cell. Mol. Life Sci.* **73**, 3075–3095
100. McCown, P. J., Ruszkowska, A., Kunkler, C. N., Breger, K., Hulewicz, J. P., Wang, M. C., *et al.* (2020) Naturally occurring modified ribonucleosides. *Wiley Interdiscip. Rev. RNA* **11**, e1595
101. Cavarelli, J., Rees, B., Ruff, M., Thierry, J. C., and Moras, D. (1993) Yeast tRNAAsp recognition by its cognate class II aminoacyl-tRNA synthetase. *Nature* **362**, 181–184
102. Ishitani, R., Nureki, O., Nameki, N., Okada, N., Nishimura, S., and Yokoyama, S. (2003) Alternative tertiary structure of tRNA for recognition by a posttranscriptional modification enzyme. *Cell* **113**, 383–394
103. Dalluge, J. J., Hashizume, T., Sopchik, A. E., McCloskey, J. A., and Davis, D. R. (1996) Conformational flexibility in RNA: the role of dihydrouridine. *Nucleic Acids Res.* **24**, 1073–1079
104. Motorin, Y., and Helm, M. (2011) RNA nucleotide methylation. *Wiley Interdiscip. Rev. RNA* **2**, 611–631
105. Davis, D. R., and Dale Poulter, C. (1991) H-15N NMR studies of Escherichia coli tRNAPhe from hisT mutants: a structural role for pseudouridine. *Biochemistry* **30**, 4223–4231
106. Kawai, G., Yamamoto, Y., Kamimura, T., Masegi, T., Sekine, M., Hata, T., *et al.* (1992) Conformational rigidity of specific pyrimidine residues in tRNA arises from posttranscriptional modifications that enhance steric interaction between the base and the 2'-hydroxyl group. *Biochemistry* **31**, 1040–1046
107. Nobles, K. N., Yarian, C. S., Liu, G., Guenther, R. H., and Agris, P. F. (2002) Highly conserved modified nucleosides influence Mg2+-dependent tRNA folding. *Nucleic Acids Res.* **30**, 4751–4760
108. Agris, P. F. (1996) The importance of being modified: roles of modified nucleosides and Mg2+ in RNA structure and function. *Prog. Nucleic Acid Res. Mol. Biol.* **53**, 79–129
109. Kowalak, J. A., Dalluge, J. J., McCloskey, J. A., and Stetter, K. O. (1994) The role of posttranscriptional modification in stabilization of transfer RNA from hyperthermophiles. *Biochemistry* **33**, 7869–7876
110. Nomura, Y., Ohno, S., Nishikawa, K., and Yokogawa, T. (2016) Correlation between the stability of tRNA tertiary structure and the catalytic efficiency of a tRNA-modifying enzyme, archaeal tRNA-guanine transglycosylase. *Genes Cells* **21**, 41–52
111. Hori, H. (2014) Methylated nucleosides in tRNA and tRNA methyltransferases. *Front. Genet.* **5**, 144
112. Ayadi, L., Galvanin, A., Pichot, F., Marchand, V., and Motorin, Y. (2019) RNA ribose methylation (2′-O-methylation): occurrence, biosynthesis and biological functions. *Biochim. Biophys. Acta Gene Regul. Mech.* **1862**, 253–269
113. Kumagai, I., Watanabe, K., and Oshima, T. (1980) Thermally induced biosynthesis of 2'-O-methylguanosine in tRNA from an extreme thermophile, Thermus thermophilus HB27. *Proc. Natl. Acad. Sci. U. S. A.* **77**, 1922–1926
114. McCloskey, J. A., Graham, D. E., Zhou, S., Crain, P. F., Ibba, M., Konisky, J., *et al.* (2001) Post-transcriptional modification in archaeal tRNAs: identities and phylogenetic relations of nucleotides from mesophilic and hyperthermophilic Methanococcales. *Nucleic Acids Res.* **29**, 4699–4706
115. Voigts-Hoffmann, F., Hengesbach, M., Kobitski, A. Y., van Aerschot, A., Herdewijn, P., Nienhaus, G. U., *et al.* (2007) A methyl group controls conformational equilibrium in human mitochondrial tRNA(Lys). *J. Am. Chem. Soc.* **129**, 13382–13383
116. Helm, M., Giegé, R., and Florentz, C. (1999) A Watson-Crick base-pair-disrupting methyl group (m1A9) is sufficient for cloverleaf folding of human mitochondrial tRNALys. *Biochemistry* **38**, 13338–13346
117. Sohm, B., Sissler, M., Park, H., King, M. P., and Florentz, C. (2004) Recognition of human mitochondrial tRNALeu(UUR) by its cognate leucyl-tRNA synthetase. *J. Mol. Biol.* **339**, 17–29
118. Wittenhagen, L. M., and Kelley, S. O. (2003) Impact of disease-related mitochondrial mutations on tRNA structure and function. *Trends Biochem. Sci.* **28**, 605–611
119. Wolfson, A. D., Khvorova, A. M., Sauter, C., Florentz, C., and Giegé, R. (1999) Mimics of yeast tRNAAsp and their recognition by aspartyl-tRNA synthetase. *Biochemistry* **38**, 11926–11932
120. Sohm, B., Frugier, M., Brulé, H., Olszak, K., Przykorska, A., and Florentz, C. (2003) Towards understanding human mitochondrial leucine aminoacylation identity. *J. Mol. Biol.* **328**, 995–1010
121. Messmer, M., Pütz, J., Suzuki, T., Suzuki, T., Sauter, C., Sissler, M., *et al.* (2009) Tertiary network in mammalian mitochondrial tRNAAsp revealed by solution probing and phylogeny. *Nucleic Acids Res.* **37**, 6881–6895
122. Jackman, J. E., Montange, R. K., Malik, H. S., and Phizicky, E. M. (2003) Identification of the yeast gene encoding the tRNA m1G methyltransferase responsible for modification at position 9. *RNA* **9**, 574–585
123. Vilardo, E., Amman, F., Toth, U., Kotter, A., Helm, M., and Rossmanith, W. (2020) Functional characterization of the human tRNA methyltransferases TRMT10A and TRMT10B. *Nucleic Acids Res.* **48**, 6157–6169
124. Agris, P. F., Sierzputowska-Gracz, H., and Smith, C. (1986) Transfer RNA contains sites of localized positive charge: carbon NMR studies of [13C] methyl-enriched Escherichia coli and yeast tRNAPhe. *Biochemistry* **25**, 5126–5131
125. Romby, P., Carbon, P., Westhof, E., Ehresmann, C., Ebel, J. P., Ehresmann, B., *et al.* (1987) Importance of conserved residues for the conformation of the t-loop in trnas. *J. Biomol. Struct. Dyn.* **5**, 669–687
126. Anderson, J., Phan, L., Cuesta, R., Carlson, B. A., Pak, M., Asano, K., *et al.* (1998) The essential Gcd10p-Gcd14p nuclear complex is required for 1-methyladenosine modification and maturation of initiator methionyl-tRNA. *Genes Dev.* **12**, 3650–3662
127. Saikia, M., Fu, Y., Pavon-Eternod, M., He, C., and Pan, T. (2010) Genome-wide analysis of N1-methyl-adenosine modification in human tRNAs. *RNA* **16**, 1317–1327
128. Oliva, R., Cavallo, L., and Tramontano, A. (2006) Accurate energies of hydrogen bonded nucleic acid base pairs and triplets in tRNA tertiary interactions. *Nucleic Acids Res.* **34**, 865–879
129. Dai, Q., Zheng, G., Schwartz, M. H., Clark, W. C., and Pan, T. (2017) Selective enzymatic demethylation of N2,N2-dimethylguanosine in RNA and its application in high-throughput tRNA sequencing. *Angew. Chem. Int. Ed. Engl.* **56**, 5017–5020
130. Purushothaman, S. K., Bujnicki, J. M., Grosjean, H., and Lapeyre, B. (2005) Trm11p and Trm112p are both required for the formation of

2-methylguanosine at position 10 in yeast tRNA. *Mol. Cell. Biol.* **25**, 4359–4370
131. Awai, T., Kimura, S., Tomikawa, C., Ochi, A., Ihsanawati, Bessho, Y., *et al.* (2009) Aquifex aeolicus tRNA (N2,N2-guanine)-dimethyltransferase (Trm1) catalyzes transfer of methyl groups not only to guanine 26 but also to guanine 27 in tRNA. *J. Biol. Chem.* **284**, 20467–20478
132. Pallan, P. S., Kreutz, C., Bosio, S., Micura, R., and Egli, M. (2008) Effects of N2,N2-dimethylguanosine on RNA structure and stability: crystal structure of an RNA duplex with tandem m2 2G:A pairs. *RNA* **14**, 2125–2135
133. Menezes, S., Gaston, K. W., Krivos, K. L., Apolinario, E. E., Reich, N. O., Sowers, K. R., *et al.* (2011) Formation of m2G6 in Methanocaldococcus jannaschii tRNA catalyzed by the novel methyltransferase Trm14. *Nucleic Acids Res.* **39**, 7641–7655
134. Edqvist, J., Stråby, K. B., and Grosjean, H. (1995) Enzymatic formation of N2,N2-dimethylguanosine in eukaryotic tRNA: importance of the tRNA architecture. *Biochimie* **77**, 54–61
135. Yang, W.-Q., Xiong, Q.-P., Ge, J.-Y., Li, H., Zhu, W.-Y., Nie, Y., *et al.* (2021) THUMPD3-TRMT112 is a m2G methyltransferase working on a broad range of tRNA substrates. *Nucleic Acids Res.* **49**, 11900–11919
136. Nishida, Y., Ohmori, S., Kakizono, R., Kawai, K., Namba, M., Okada, K., *et al.* (2022) Required elements in tRNA for methylation by the eukaryotic tRNA (guanine-N2-) methyltransferase (Trm11-Trm112 complex). *Int. J. Mol. Sci.* **23**, 4046
137. Steinberg, S., and Cedergren, R. (1995) A correlation between N2-dimethylguanosine presence and alternate tRNA conformers. *RNA* **1**, 886–891
138. Sonawane, K. D., Bavi, R. S., Sambhare, S. B., and Fandilolu, P. M. (2016) Comparative structural dynamics of tRNAPhe with respect to hinge region methylated guanosine: a computational approach. *Cell Biochem. Biophys.* **74**, 157–173
139. Jantsch, M. F., Quattrone, A., O'Connell, M., Helm, M., Frye, M., Macias-Gonzales, M., *et al.* (2018) Positioning Europe for the EPI-TRANSCRIPTOMICS challenge. *RNA Biol.* **15**, 829–831
140. Davanloo, P., Sprinzl, M., Watanabe, K., Albani, M., and Kersten, H. (1979) Role of ribothymidine in the thermal stability of transfer RNA as monitored by proton magnetic resonance. *Nucleic Acids Res.* **6**, 1571–1581
141. Levitt, M. (1969) Detailed molecular model for transfer ribonucleic acid. *Nature* **224**, 759–763
142. Alexandrov, A., Chernyakov, I., Gu, W., Hiley, S. L., Hughes, T. R., Grayhack, E. J., *et al.* (2006) Rapid tRNA decay can result from lack of nonessential modifications. *Mol. Cell* **21**, 87–96
143. Davis, D. R. (1995) Stabilization of RNA stacking by pseudouridine. *Nucleic Acids Res.* **23**, 5020–5026
144. Charette, M., and Gray, M. W. (2000) Pseudouridine in RNA: what, where, how, and why. *IUBMB Life* **49**, 341–351
145. Lin, T. Y., Mehta, R., and Glatt, S. (2021) Pseudouridines in RNAs: switching atoms means shifting paradigms. *FEBS Lett.* **595**, 2310–2322
146. Kierzek, E., Malgowska, M., Lisowiec, J., Turner, D. H., Gdaniec, Z., and Kierzek, R. (2014) The contribution of pseudouridine to stabilities and structure of RNAs. *Nucleic Acids Res.* **42**, 3492–3501
147. Hudson, G. A., Bloomingdale, R. J., and Znosko, B. M. (2013) Thermodynamic contribution and nearest-neighbor parameters of pseudouridine-adenosine base pairs in oligoribonucleotides. *RNA* **19**, 1474–1482
148. Westhof, E., and Auffinger, P. (2012) Transfer RNA structure. In: *eLS.* Wiley, Hoboken, NJ
149. Sundaralingam, M., Rao, S. T., and Abola, J. (1971) Molecular conformation of dihydrouridine: puckered base nucleoside of transfer RNA. *Science* **172**, 725–727
150. Suck, D., Saenger, W., and Zechmeister, K. (1971) Conformation of the tRNA minor constituent dihydrouridine. *FEBS Lett.* **12**, 257–259
151. Stuart, J. W., Basti, M. M., Smith, W. S., Forrest, B., Guenther, R., Sierzputowska-Gracz, H., *et al.* (1996) Structure of the trinucleotide D-acp3U-A with coordinated Mg2+ demonstrates that modified nucleosides contribute to regional conformations of RNA. *Nucleos. Nucleot.* **15**, 1009–1028
152. Dyubankova, N., Sochacka, E., Kraszewska, K., Nawrot, B., Herdewijn, P., and Lescrinier, E. (2015) Contribution of dihydrouridine in folding of the D-arm in tRNA. *Org. Biomol. Chem.* **13**, 4960–4966
153. Kimura, S., and Waldor, M. K. (2019) The RNA degradosome promotes tRNA quality control through clearance of hypomodified tRNA. *Proc. Natl. Acad. Sci. U. S. A.* **116**, 1394–1403
154. Davis, D. R., Griffey, R. H., and Yamaizumi, Z. (1986) 15N-labeled tRNA. Identification of dihydrouridine in Escherichia coli tRNAfMet, tRNALys, and tRNAPhe by 1H-15N two-dimensional NMR. *J. Biol. Chem.* **261**, 3584–3587
155. Friedman, S., Li, H. J., Nakanishi, K., and Van Lear, G. (1974) 3-(3-amino-3-carboxypropyl)uridine. The structure of the nucleoside in Escherichia coli transfer ribonucleic acid that reacts with phenoxyacetoxysuccinimide. *Biochemistry* **13**, 2932–2937
156. Friedman, S. (1979) The effect of chemical modification of 3-(3-amino-3-carboxypropyl)uridine on tRNA function. *J. Biol. Chem.* **254**, 7111–7115
157. Ohashi, Z., Maeda, M., McCloskey, J. A., and Nishimura, S. (1974) 3-(3-Amino-3-Carboxypropyl)uridine. Novel modified nucleoside isolated from Escherichia coli phenylalanine transfer ribonucleic acid. *Biochemistry* **13**, 2620–2625
158. Johnson, G. D., Pirtle, I. L., and Pirtle, R. M. (1985) The nucleotide sequence of tyrosine tRNAQ*ΨA from bovine liver. *Arch. Biochem. Biophys.* **236**, 448–453
159. Barciszewska, M., Dirheimer, G., and Keith, G. (1983) The nucleotide sequence of methionine elongator tRNA from wheat germ. *Biochem. Biophys. Res. Commun.* **114**, 1161–1168
160. Takakura, M., Ishiguro, K., Akichika, S., Miyauchi, K., and Suzuki, T. (2019) Biogenesis and functions of aminocarboxypropyluridine in tRNA. *Nat. Commun.* **10**, 5542
161. Meyer, B., Immer, C., Kaiser, S., Sharma, S., Yang, J., Watzinger, P., *et al.* (2020) Identification of the 3-amino-3-carboxypropyl (acp) transferase enzyme responsible for acp3U formation at position 47 in Escherichia coli tRNAs. *Nucleic Acids Res.* **48**, 1435–1450
162. Barraud, P., Gato, A., Heiss, M., Catala, M., Kellner, S., and Tisné, C. (2019) Time-resolved NMR monitoring of tRNA maturation. *Nat. Commun.* **10**, 3373
163. Schultz, S. K. L., and Kothe, U. (2020) tRNA elbow modifications affect the tRNA pseudouridine synthase TruB and the methyltransferase TrmA. *RNA* **26**, 1131–1142
164. Novoa, E. M., Pavon-Eternod, M., Pan, T., and Ribas de Pouplana, L. (2012) A role for tRNA modifications in genome structure and codon usage. *Cell* **149**, 202–213
165. Yu, F., Tanaka, Y., Yamashita, K., Suzuki, T., Nakamura, A., Hirano, N., *et al.* (2011) Molecular basis of dihydrouridine formation on tRNA. *Proc. Natl. Acad. Sci. U. S. A.* **108**, 19593–19598
166. Liu, R.-J., Long, T., Li, J., Li, H., and Wang, E.-D. (2017) Structural basis for substrate binding and catalytic mechanism of a human RNA: m5C methyltransferase NSun6. *Nucleic Acids Res.* **45**, 6684–6697
167. Finer-Moore, J., Czudnochowski, N., O'Connell, J. D., Wang, A. L., and Stroud, R. M. (2015) Crystal structure of the human tRNA m1A58 methyltransferase-tRNA3Lys complex: refolding of substrate tRNA allows access to the methylation target. *J. Mol. Biol.* **427**, 3862–3876
168. Osawa, T., Kimura, S., Terasaka, N., Inanaga, H., Suzuki, T., and Numata, T. (2011) Structural basis of tRNA agmatinylation essential for AUA codon decoding. *Nat. Struct. Mol. Biol.* **18**, 1275–1280
169. Wang, C., Jia, Q., Zeng, J., Chen, R., and Xie, W. (2017) Structural insight into the methyltransfer mechanism of the bifunctional Trm5. *Sci. Adv.* **3**, e1700195
170. Schwalm, E. L., Grove, T. L., Booker, S. J., and Boal, A. K. (2016) Crystallographic capture of a radical S-adenosylmethionine enzyme in the act of modifying tRNA. *Science* **352**, 309–312
171. Beenstock, J., Ona, S. M., Porat, J., Orlicky, S., Wan, L. C. K., Ceccarelli, D. F., *et al.* (2020) A substrate binding model for the KEOPS tRNA modifying complex. *Nat. Commun.* **11**, 6233

172. Beenstock, J., and Sicheri, F. (2021) The structural and functional workings of KEOPS. *Nucleic Acids Res.* **49**, 10818–10834
173. Sievers, K., Welp, L., Urlaub, H., and Ficner, R. (2021) Structural and functional insights into human tRNA guanine transgylcosylase. *RNA Biol.* **18**, 382–396
174. Dolce, L. G., Zimmer, A. A., Tengo, L., Weis, F., Rubio, M. A. T., Alfonzo, J. D., *et al.* (2022) Structural basis for sequence-independent substrate selection by eukaryotic wobble base tRNA deaminase ADAT2/3. *Nat. Commun.* **13**, 6737
175. Ruiz-Arroyo, V. M., Raj, R., Babu, K., Onolbaatar, O., Roberts, P. H., and Nam, Y. (2023) Structures and mechanisms of tRNA methylation by METTL1–WDR4. *Nature* **613**, 383–390
176. Li, J., Wang, L., Hahn, Q., Nowak, R. P., Viennet, T., Orellana, E. A., *et al.* (2023) Structural basis of regulated m7G tRNA modification by METTL1–WDR4. *Nature* **613**, 391–397
177. Kojic, M., Gawda, T., Gaik, M., Begg, A., Salerno-Kochan, A., Kurniawan, N. D., *et al.* (2021) Elp2 mutations perturb the epitranscriptome and lead to a complex neurodevelopmental phenotype. *Nat. Commun.* **12**, 19
178. Jaciuk, M., Scherf, D., Kaszuba, K., Gaik, M., Rau, A., Kościelniak, A., *et al.* (2023) Cryo-EM structure of the fully assembled Elongator complex. *Nucleic Acids Res.* **51**, 2011–2032
179. Lin, T.-Y., Abbassi, N. E. H., Zakrzewski, K., Chramiec-Głąbik, A., Jemioła-Rzemińska, M., Różycki, J., *et al.* (2019) The Elongator subunit Elp3 is a non-canonical tRNA acetyltransferase. *Nat. Commun.* **10**, 1–12
180. Kuhle, B., Lander, G. C., Hirschi, M., Doerfel, L. K., Lander, G. C., and Schimmel, P. (2022) Structural basis for shape-selective recognition and aminoacylation of a D-armless human mitochondrial tRNA. *Nat. Commun.* **13**, 1–12
181. Stephen, P., Ye, S., Zhou, M., Song, J., Zhang, R., Wang, E. D., *et al.* (2018) Structure of Escherichia coli arginyl-tRNA synthetase in complex with tRNAArg: pivotal role of the D-loop. *J. Mol. Biol.* **430**, 1590–1606
182. Yu, Z., Wu, Z., Li, Y., Hao, Q., Cao, X., Blaha, G. M., *et al.* (2023) Structural basis of a two-step tRNA recognition mechanism for plastid glycyl-tRNA synthetase. *Nucleic Acids Res.* **51**, 4000–4011
183. Han, L., Luo, Z., Ju, Y., Chen, B., Zou, T., Wang, J., *et al.* (2023) The binding mode of orphan glycyl-tRNA synthetase with tRNA supports the synthetase classification and reveals large domain movements. *Sci. Adv.* **9**, eadf1027
184. Wu, J., Niu, S., Tan, M., Huang, C., Li, M., Song, Y., *et al.* (2018) Cryo-EM structure of the human ribonuclease P holoenzyme. *Cell* **175**, 1393–1404.e11
185. Zhang, X., Yang, F., Zhan, X., Bian, T., Xing, Z., Lu, Y., *et al.* (2023) Structural basis of pre-tRNA intron removal by human tRNA splicing endonuclease. *Mol. Cell* **83**, 1328–1339.e4
186. Sekulovski, S., Sušac, L., Stelzl, L. S., Tampé, R., and Trowitzsch, S. (2023) Structural basis of substrate recognition by human tRNA splicing endonuclease TSEN. *Nat. Struct. Mol. Biol.* **30**, 834–840
187. Hayne, C. K., Butay, K. J. U., Stewart, Z. D., Krahn, J. M., Perera, L., Williams, J. G., *et al.* (2023) Structural basis for pre-tRNA recognition and processing by the human tRNA splicing endonuclease complex. *Nat. Struct. Mol. Biol.* **30**, 824–833
188. Byrne, R. T., Jenkins, H. T., Peters, D. T., Whelan, F., Stowell, J., Aziz, N., *et al.* (2015) Major reorientation of tRNA substrates defines specificity of dihydrouridine synthases. *Proc. Natl. Acad. Sci. U. S. A.* **112**, 6033–6037
189. Dauden, M. I., Jaciuk, M., Weis, F., Lin, T. Y., Kleindienst, C., Abbassi, N. E. H., *et al.* (2019) Molecular basis of tRNA recognition by the Elongator complex. *Sci. Adv.* **5**, 1–14
190. Zhang, J. (2021) Interplay between host trnas and hiv-1: a structural perspective. *Viruses* **13**, 1–14
191. Bou-Nader, C., Muecksch, F., Brown, J. B., Gordon, J. M., York, A., Peng, C., *et al.* (2021) HIV-1 matrix-tRNA complex structure reveals basis for host control of Gag localization. *Cell Host Microbe* **29**, 1421–1436.e7
192. Liu, Y., Strugatsky, D., Liu, W., and Zhou, Z. H. (2021) Structure of human cytomegalovirus virion reveals host tRNA binding to capsid-associated tegument protein pp150. *Nat. Commun.* **12**, 1–9
193. Lezzhov, A. A., Atabekova, A. K., Tolstyko, E. A., and Lazareva, E. A. (2019) Plant science RNA phloem transport mediated by pre-miRNA and viral tRNA-like structures. *Plant Sci.* **284**, 99–107
194. Khan, S. Y., Hackett, S. F., and Riazuddin, S. A. (2016) Non-coding RNA profiling of the developing murine lens. *Exp. Eye Res.* **145**, 347–351
195. Colussi, T. M., Costantino, D. A., Hammond, J. A., Ruehle, G. M., Nix, J. C., and Kieft, J. S. (2014) The structural basis of transfer RNA mimicry and conformational plasticity by a viral RNA. *Nature* **511**, 366–369
196. Boehringer, D., Thermann, R., Ostareck-Lederer, A., Lewis, J. D., and Stark, H. (2005) Structure of the hepatitis C virus IRES bound to the human 80S ribosome: remodeling of the HCV IRES. *Structure* **13**, 1695–1706
197. Jones, C. P., Cantara, W. A., Olson, E. D., and Musier-Forsyth, K. (2014) Small-angle X-ray scattering-derived structure of the HIV-1 5′ UTR reveals 3D tRNA mimicry. *Proc. Natl. Acad. Sci. U. S. A.* **111**, 3395–3400
198. Tsai, C. H., and Dreher, T. W. (1991) Turnip yellow mosaic virus RNAs with anticodon loop substitutions that result in decreased valylation fail to replicate efficiently. *J. Virol.* **65**, 3060–3067
199. Matsuda, D., Dunoyer, P., Hemmer, O., Fritsch, C., and Dreher, T. W. (2000) The valine anticodon and valylatability of peanut clump virus RNAs are not essential but provide a modest competitive advantage in plants. *J. Virol.* **74**, 8720–8725
200. Vieweger, M., Holmstrom, E. D., and Nesbitt, D. J. (2015) Single-molecule FRET reveals three conformations for the TLS domain of Brome mosaic virus genome. *Biophys. J.* **109**, 2625–2636
201. Bonilla, S. L., Sherlock, M. E., MacFadden, A., and Kieft, J. S. (2021) A viral RNA hijacks host machinery using dynamic conformational changes of a tRNA-like structure. *Science* **374**, 955–960
202. Kuhn, C., Wilusz, J. E., Zheng, Y., Beal, P. A., and Joshua, L. (2015) On-enzyme refolding permits small RNA and tRNA surveillance by the CCA-adding enzyme. *Cell* **160**, 644–658
203. Lu, X., Huang, J., Wu, S., Zheng, Q., Fu, H., Xi, Q., *et al.* (2020) The tRNA-like small noncoding RNA mascRNA promotes global protein translation. *EMBO Rep.* **21**, 1–17
204. Levi, O., and Arava, Y. (2019) mRNA association by aminoacyl tRNA synthetase occurs at a putative anticodon mimic and autoregulates translation in response to tRNA levels. *PLoS Biol.* **17**, 1–24
205. Wang, W., Chen, X., Wolin, S. L., and Xiong, Y. (2018) Structural basis for tRNA mimicry by a bacterial Y RNA. *Structure* **26**, 1635–1644.e3
206. Telonis, A. G., Loher, P., Kirino, Y., and Rigoutsos, I. (2014) Nuclear and mitochondrial tRNA-lookalikes in the human genome. *Front. Genet.* **5**, 1–11
207. Hoser, S. M., Hoffmann, A., Meindl, A., Gamper, M., Fallmann, J., Bernhart, S. H., *et al.* (2020) Intronic tRNAs of mitochondrial origin regulate constitutive and alternative splicing. *Genome Biol.* **21**, 299
208. Kreuzer, K. D., and Henkin, T. M. (2018) The T-box riboswitch: tRNA as an effector to modulate gene regulation. *Microbiol. Spectr.* **6**, 10–1128
209. Marchand, J. A., Pierson Smela, M. D., Jordan, T. H. H., Narasimhan, K., and Church, G. M. (2021) TBDB: a database of structurally annotated T-box riboswitch:tRNA pairs. *Nucleic Acids Res.* **49**, D229–D235
210. Zhang, J. (2020) Unboxing the T-box riboswitches—A glimpse into multivalent and multimodal RNA–RNA interactions. *Wiley Interdiscip. Rev. RNA* **11**, 1–21
211. Li, S., Su, Z., Lehmann, J., Stamatopoulou, V., Giarimoglou, N., Henderson, F. E., *et al.* (2019) Structural basis of amino acid surveillance by higher-order tRNA-mRNA interactions. *Nat. Struct. Mol. Biol.* **26**, 1094–1105
212. Zhang, J., Chetnani, B., Cormack, E. D., Alonso, D., Liu, W., Mondragón, A., *et al.* (2018) Specific structural elements of the t-box riboswitch drive the two-step binding of the tRNA ligand. *Elife* **7**, 1–22
213. Battaglia, R. A., Grigg, J. C., and Ke, A. (2019) Structural basis for tRNA decoding and aminoacylation sensing by T-box riboregulators. *Nat. Struct. Mol. Biol.* **26**, 1106–1113
214. Suddala, K. C., and Zhang, J. (2019) High-affinity recognition of specific tRNAs by an mRNA anticodon-binding groove. *Nat. Struct. Mol. Biol.* **26**, 1114–1122
215. Kasai, H., Nakanishi, K., Macfarlane, R. D., Torgerson, D. F., Ohashi, Z., McCloskey, J. A., *et al.* (1976) The structure of Q* nucleoside isolated

from rabbit liver transfer ribonucleic acid. *J. Am. Chem. Soc.* **98**, 5044–5046
216. Zhang, W., Xu, R., Matuszek, Z. A., Cai, Z., and Pan, T. (2020) Detection and quantification of glycosylated queuosine modified tRNAs by acid denaturing and APB gels. *RNA* **26**, 1291–1298
217. Thumbs, P., Ensfelder, T. T., Hillmeier, M., Wagner, M., Heiss, M., Scheel, C., *et al.* (2020) Synthesis of galactosyl-queuosine and distribution of hypermodified Q-nucleosides in mouse tissues. *Angew. Chem. Int. Ed. Engl.* **59**, 12352–12356
218. Hillmeier, M., Wagner, M., Ensfelder, T., Korytiakova, E., Thumbs, P., Müller, M., *et al.* (2021) Synthesis and structure elucidation of the human tRNA nucleoside mannosyl-queuosine. *Nat. Commun.* **12**, 7123
219. Flynn, R. A., Pedram, K., Malaker, S. A., Batista, P. J., Smith, B. A. H., Johnson, A. G., *et al.* (2021) Small RNAs are modified with N-glycans and displayed on the surface of living cells. *Cell* **184**, 3109–3124.e22
220. Okimoto, R., and Wolstenholme, D. R. (1990) A set of tRNAs that lack either the TψC arm or the dihydrouridine arm: towards a minimal tRNA adaptor. *EMBO J.* **9**, 3405–3411
221. Pons, J., Bover, P., Bidegaray-batista, L., and Arnedo, M. A. (2019) Armless mitochondrial tRNAs conserved for over 30 millions of years in spiders. *BMC Genomics* **20**, 665
222. Sprinzl, M., and Vassilenko, K. S. (2005) Compilation of tRNA sequences and sequences of tRNA genes. *Nucleic Acids Res.* **33**, D139–D140
223. Sakurai, M., Ohtsuki, T., and Watanabe, K. (2005) Modification at position 9 with 1-methyladenosine is crucial for structure and function of nematode mitochondrial tRNAs lacking the entire T-arm. *Nucleic Acids Res.* **33**, 1653–1661
224. Jühling, T., Duchardt-Ferner, E., Bonin, S., Wöhnert, J., Pütz, J., Florentz, C., *et al.* (2018) Small but large enough: structural properties of armless mitochondrial tRNAs from the nematode Romanomermis culicivorax. *Nucleic Acids Res.* **46**, 9170–9180
225. Wende, S., Platzer, E. G., Jühling, F., Pütz, J., Florentz, C., Stadler, P. F., *et al.* (2014) Biochimie biological evidence for the world's smallest tRNAs. *Biochimie* **100**, 151–158
226. Hennig, O., Philipp, S., Bonin, S., Rollet, K., Kolberg, T., Jühling, T., *et al.* (2020) Adaptation of the romanomermis culicivorax CCA-adding enzyme to miniaturized armless tRNA substrates. *Int. J. Mol. Sci.* **21**, 9047
227. Sakurai, M., Watanabe, Y., Watanabe, K., and Ohtsuki, T. (2006) A protein extension to shorten RNA : elongated elongation factor-Tu recognizes the D-arm of T-armless tRNAs in nematode mitochondria. *Biochem. J.* **256**, 249–256
228. Suematsu, T., Sato, A., Sakurai, M., Watanabe, K., and Ohtsuki, T. (2005) A unique tRNA recognition mechanism of Caenorhabditis elegans mitochondrial EF-Tu2. *Nucleic Acids Res.* **33**, 4683–4691
229. de Bruijn, M. H., and Klug, A. (1983) A model for the tertiary structure of mammalian mitochondrial transfer RNAs lacking the entire "dihydrouridine" loop and stem. *EMBO J.* **2**, 1309–1321
230. Tuppen, H. A. L., Naess, K., Kennaway, N. G., Al-Dosary, M., Lesko, N., Yarham, J. W., *et al.* (2012) Mutations in the mitochondrial tRNA Ser(AGY) gene are associated with deafness, retinal degeneration, myopathy and epilepsy. *Eur. J. Hum. Genet.* **20**, 897–904
231. Yu, T., Zhang, Y. Y., Zheng, W.-Q., Wu, S., Li, G., Zhang, Y. Y., *et al.* (2022) Selective degradation of tRNASer(AGY) is the primary driver for mitochondrial seryl-tRNA synthetase-related disease. *Nucleic Acids Res.* **50**, 11755–11774
232. Eggertsson, G., and Söll, D. (1988) Transfer ribonucleic acid-mediated suppression of termination codons in Escherichia coli. *Microbiol. Rev.* **52**, 354–374
233. Kachale, A., Pavlíková, Z., Nenarokova, A., Roithová, A., Durante, I. M., Miletínová, P., *et al.* (2023) Short tRNA anticodon stem and mutant eRF1 allow stop codon reassignment. *Nature* **613**, 751–758
234. Lueck, J. D., Yoon, J. S., Perales-Puchalt, A., Mackey, A. L., Infield, D. T., Behlke, M. A., *et al.* (2019) Engineered transfer RNAs for suppression of premature termination codons. *Nat. Commun.* **10**, 1–11
235. Ogawa, A., Hayami, M., Sando, S., and Aoyama, Y. (2012) A concept for selection of codon-suppressor tRNAs based on read-through ribosome display in an *in vitro* compartmentalized cell-free translation system. *J. Nucleic Acids* **2012**, 538129
236. Lin, T.-Y. Y., and Glatt, S. (2022) ACEing premature codon termination using anticodon-engineered sup-tRNA-based therapy. *Mol. Ther. Nucleic Acids* **29**, 368–369
237. Cummins, C. M., Culbertson, M. R., and Knapp, G. (1985) Frameshift suppressor mutations outside the anticodon in yeast proline tRNAs containing an intervening sequence. *Mol. Cell. Biol.* **5**, 1760–1771
238. Atkins, J. F., and Björk, G. R. (2009) A gripping tale of ribosomal frameshifting: extragenic suppressors of frameshift mutations spotlight P-site realignment. *Microbiol. Mol. Biol. Rev.* **73**, 178–210
239. Maehigashi, T., Dunkle, J. A., Miles, S. J., and Dunham, C. M. (2014) Structural insights into +1 frameshifting promoted by expanded or modification-deficient anticodon stem loops. *Proc. Natl. Acad. Sci. U. S. A.* **111**, 12740–12745
240. Qian, Q., Li, J. N., Zhao, H., Hagervall, T. G., Farabaugh, P. J., and Björk, G. R. (1998) A new model for phenotypic suppression of frameshift mutations by mutant tRNAs. *Mol. Cell.* **1**, 471–482
241. Hong, S., Sunita, S., Maehigashi, T., Hoffer, E. D., Dunkle, J. A., and Dunham, C. M. (2018) Mechanism of tRNA-mediated +1 ribosomal frameshifting. *Proc. Natl. Acad. Sci. U. S. A.* **115**, 11226–11231
242. Fagan, C. E., Maehigashi, T., Dunkle, J. A., Miles, S. J., and Dunham, C. M. (2014) Structural insights into translational recoding by frameshift suppressor tRNASufJ. *RNA* **20**, 1944–1954
243. Gamper, H., Mao, Y., Masuda, I., McGuigan, H., Blaha, G., Wang, Y., *et al.* (2021) Twice exploration of tRNA +1 frameshifting in an elongation cycle of protein synthesis. *Nucleic Acids Res.* **49**, 10046–10060
244. Demo, G., Gamper, H. B., Loveland, A. B., Masuda, I., Carbone, C. E., Svidritskiy, E., *et al.* (2021) Structural basis for +1 ribosomal frameshifting during EF-G-catalyzed translocation. *Nat. Commun.* **12**, 1–12
245. Wang, K., Schmied, W. H., and Chin, J. W. (2012) Reprogramming the genetic code: from triplet to quadruplet codes. *Angew. Chem. Int. Ed. Engl.* **51**, 2288–2297
246. Ponchon, L., and Dardel, F. (2007) Recombinant RNA technology: the tRNA scaffold. *Nat. Methods* **4**, 571–576
247. Lee, E., Bujalowski, P. J., Teramoto, T., Gottipati, K., Scott, S. D., Padmanabhan, R., *et al.* (2021) Structures of flavivirus RNA promoters suggest two binding modes with NS5 polymerase. *Nat. Commun.* **12**, 1–12
248. Fahmi, N. E., Dedkova, L., Wang, B., Golovine, S., Hecht, S. M., and Charlottes, V. (2007) Site-specific incorporation of glycosylated serine and tyrosine derivatives into proteins. *J. Am. Chem. Soc.* **129**, 3586–3597
249. Porter, J. J., Heil, C. S., and Lueck, J. D. (2021) Therapeutic promise of engineered nonsense suppressor tRNAs. *Wiley Interdiscip. Rev. RNA* **12**, 1–27
250. Ko, W., Porter, J. J., Sipple, M. T., Edwards, K. M., and Lueck, J. D. (2022) Efficient suppression of endogenous CFTR nonsense mutations using anticodon-engineered transfer RNAs. *Mol. Ther. Nucleic Acids* **28**, 685–701
251. Wang, J., Zhang, Y., Mendonca, C. A., Yukselen, O., Muneeruddin, K., Ren, L., *et al.* (2022) AAV-delivered suppressor tRNA overcomes a nonsense mutation in mice. *Nature* **604**, 343–348
252. Kappel, K., Zhang, K., Su, Z., Watkins, A. M., Kladwang, W., Li, S., *et al.* (2020) Accelerated cryo-EM-guided determination of three-dimensional RNA-only structures. *Nat. Methods* **17**, 699–707
253. Jumper, J., Evans, R., Pritzel, A., Green, T., Figurnov, M., Ronneberger, O., *et al.* (2021) Highly accurate protein structure prediction with AlphaFold. *Nature* **596**, 583–589
254. Monsen, R. C., Chua, E. Y. D., Hopkins, J. B., Chaires, J. B., and Trent, J. O. (2023) Structure of a 28.5 kDa duplex-embedded G-quadruplex system resolved to 7.4 Å resolution with cryo-EM. *Nucleic Acids Res.* **51**, 1–17
255. Kaymak, E., and Rando, O. J. (2023) Staying together after the breakup: tRNA halves in extracellular fluids. *Proc. Natl. Acad. Sci. U. S. A.* **120**, 10–12
256. Chen, X., and Wolin, S. L. (2023) Transfer RNA halves are found as nicked tRNAs in cells: evidence that nicked tRNAs regulate expression of an RNA repair operon. *RNA* **29**, 620–629

257. Chen, L., Xu, W., Liu, K., Jiang, Z., Han, Y., Jin, H., *et al.* (2021) 5′ Half of specific tRNAs feeds back to promote corresponding tRNA gene transcription in vertebrate embryos. *Sci. Adv.* **7**, eabh0494
258. Bayazit, M. B., Jacovetti, C., Cosentino, C., Sobel, J., Wu, K., Brozzi, F., *et al.* (2022) Small RNAs derived from tRNA fragmentation regulate the functional maturation of neonatal β cells. *Cell Rep.* **40**, 111069
259. Catala, M., Gato, A., Tisné, C., and Barraud, P. (2020) 1H, 15N chemical shift assignments of the imino groups of yeast tRNAPhe: influence of the post-transcriptional modifications. *Biomol. NMR Assign.* **14**, 169–174
260. Laxman, S., Sutter, B. M., Wu, X., Kumar, S., Guo, X., Trudgian, D. C., *et al.* (2013) Sulfur amino acids regulate translational capacity and metabolic homeostasis through modulation of tRNA thiolation. *Cell* **154**, 416–429
261. Tuorto, F., Legrand, C., Cirzi, C., Federico, G., Liebers, R., Müller, M., *et al.* (2018) Queuosine-modified tRNAs confer nutritional control of protein translation. *EMBO J.* **37**, e99777
262. Liu, F., Clark, W., Luo, G., Wang, X., Fu, Y., Wei, J., *et al.* (2016) ALKBH1-mediated tRNA demethylation regulates translation. *Cell* **167**, 816–828.e16